
Sentinel 3
SLSTR
SLSTR B FPA Spectral Calibration Report

	Name	Signature / Date
Prepared by	Tim Nightingale	
Checked by	Dave Smith	
Project Manager	Brian Maddison	
PA Manager	Richard Stamper	

Science and Technology Facilities Council
Rutherford Appleton Laboratory
Harwell Science and Innovation Campus
Didcot
Oxfordshire OX11 0QX
United Kingdom

DISTRIBUTION

Name	Organisation
Brian Maddison	RAL
Chris Mutlow	RAL
Dion Dawson	RAL
Dan Peters	RAL
Daniel Gandolfo	RAL
Mireya Etxaluze	RAL
Edward Polehampton	RAL
Fabio Brandini	Selex ES
Massimo Cosi	Selex ES
Gianna Gironi	Selex ES
Giada Miogrossi	Selex ES
Alessandro Dattolo	Selex ES
Marc Barillot	Thales Alenia
Stephane Bianchi	Thales Alenia
Johannes Frerick	ESA
Jens Nieke	ESA



CHANGE LOG

Date	Issue	Revision	Pages	Reason for change
28-01-2015	0.1	0		First draft issue
27-02-2015	0.2	0		Added URD templates to 87K measurements, temperature sensitivity section, out-of-band response section, S8, S9 slope section, conclusions section, compliance matrix.
29-06-2015	1.0	0		First official release. Added note to Section 8.4 clarifying the operating temperatures of the detectors in channels S1, S2 and S3.

CONTENTS

1 Scope of Document / Introduction	6
2 Abbreviations	6
3 Applicable Documents	6
4 Reference Documents	7
5 Introduction	8
6 Experimental setup	9
6.1 FPA	10
6.1.1 Assembly and integration.....	10
6.1.2 Vacuum procedure.....	10
6.1.3 Cooling procedure.....	10
6.1.4 EGSE	10
6.2 FTS.....	10
6.2.1 FTS final optics	10
6.2.2 FTS operations	11
6.2.3 FPA analogue measurements	11
6.2.4 "Turn-and-turn-about" measurements.....	12
7 Theoretical basis.....	13
7.1 FPA spectral response.....	13
7.2 Uncertainties in FPA spectral response.....	13
7.3 Additional optical elements	14
7.4 Uncertainties due to additional optical elements	14
7.5 FTS relative spectral transmission	14
7.6 Uncertainties in FTS relative spectral transmission	15
7.7 Spectral transmission of an optical element	15
7.8 Uncertainties in the spectral transmission of an optical element	16
8 Measurements	17
8.1 Detector measurements.....	17
8.1.1 Silicon diode detector (Bruker ID510/8, S/N 172)	17
8.1.2 Silicon diode detector (Bruker ID510/8, S/N 182)	18
8.1.3 DLATGS detector (Bruker ID301/8, S/N 7083)	19
8.1.4 DLATGS detector (Bruker ID301/8, S/N 8014)	20
8.2 FTS relative spectral transmission	21
8.2.1 FTS visible relative spectral transmission (S1 – S3).....	22
8.2.2 FTS SWIR relative transmission (S4 – S7).....	23
8.2.3 FTS TIR relative transmission (S7 – S9)	24
8.3 Neutral density filters and out-of-band filters.....	25
8.3.1 0.1% SWIR neutral density filter (Thorlabs NENIR30B)	26
8.3.2 1% SWIR neutral density filter (Thorlabs NENIR20B)	27
8.3.3 1% TIR neutral density filter (Thorlabs NDIR20B)	28
8.4 FPA unpolarised spectral response at 87K	29
8.4.1 S1 unpolarised spectral response at 87K	30
8.4.2 S2 unpolarised spectral response at 87K	31
8.4.3 S3 unpolarised spectral response at 87K	32

8.4.4	S4 unpolarised spectral response at 87K	33
8.4.5	S5 unpolarised spectral response at 87K	34
8.4.6	S6 unpolarised spectral response at 87K	35
8.4.7	S7 unpolarised spectral response at 87K	36
8.4.8	S8 unpolarised spectral response at 87K	37
8.4.9	S9 unpolarised spectral response at 87K	38
8.5	FPA unpolarised spectral response temperature sensitivity	39
8.5.1	S1 unpolarised spectral response temperature sensitivity.....	39
8.5.2	S2 unpolarised spectral response temperature sensitivity.....	40
8.5.3	S3 unpolarised spectral response temperature sensitivity.....	41
8.5.4	S4 unpolarised spectral response temperature sensitivity.....	42
8.5.5	S5 unpolarised spectral response temperature sensitivity.....	43
8.5.6	S6 unpolarised spectral response temperature sensitivity.....	44
8.5.7	S7 unpolarised spectral response temperature sensitivity.....	45
8.5.8	S8 unpolarised spectral response temperature sensitivity.....	46
8.5.9	S9 unpolarised spectral response temperature sensitivity.....	47
8.6	FPA unpolarised out-of-band responses at 87K	49
8.7	S8 longwave and S9 shortwave slopes at 87K	50
9	Conclusions.....	51
9.1	Lessons learned	51
9.2	Outstanding work	52
10	Compliance matrix	53
11	Appendix.....	56
11.1	File naming	56
11.1.1	FEE binary spectrogram file.....	56
11.1.2	FEE ASCII spectrogram file	57
11.1.3	Brucker OPUS spectrogram file	58
11.1.4	National Instruments TDMS synchronisation file	59
11.1.5	National Instruments netCDF synchronisation file	59



1 Scope of Document / Introduction

This document describes the spectral response calibration of the SLSTR B (Sentinel-3A) Focal Plane Assembly (FPA), performed at the Rutherford Appleton Laboratory in July 2014.

2 Abbreviations

CCA	Cryocooler Assembly
EGSE	Electrical Ground Support Equipment
FPA	Focal Plane Assembly
FTS	Fourier Transform Spectrometer
NPL	National Physical Laboratory, UK
RAL	STFC Rutherford Appleton Laboratory, UK
SLSTR	Sea and Land Surface Temperature Radiometer
STFC	Science and Technology Facilities Council
SWIR	Shortwave Infrared
TIR	Thermal Infrared
UK	United Kingdom
URD	User Requirements Document

3 Applicable Documents

The applicable documents are:

	Document title	Document reference
AD 1	SLSTR spectral response characterisation plan	S3-PL-RAL-SL-014
AD 2	SLSTR spectral calibration procedure	S3-PR-RAL-SL-003
AD 3	SENTINEL-3 SLSTR Requirements Specification	S3-RS-TAF-SL-00205
AD 4		

4 Reference Documents

The reference documents are:

	Document title	Document reference
RD 1	Certificate of calibration: Silicon detector, serial number 172, relative spectral responsivity	2013040471/3/B
RD 2	Certificate of calibration: Silicon detector, serial number 182, relative spectral responsivity	2013040471/3/A
RD 3	Certificate of calibration: DLATGS pyroelectric detector, ID 301/8 S/N: 7083, relative spectral responsivity	2013040471/2/B
RD 4	Certificate of calibration: DLATGS pyroelectric detector, ID 301/8 S/N: 8014, relative spectral responsivity	2013040471/2/A
RD 5	Spectrometer Calibration Certificates	S3-RP-RAL-SL-099

5 Introduction

This document describes the spectral response calibration of the SLSTR B (Sentinel-3A) Focal Plane Assembly (FPA), performed at the Rutherford Appleton Laboratory (RAL) in July 2014.

In a departure from traditional techniques, the FPA was illuminated by a Fourier Transform Spectrometer (FTS), rather than a grating monochromator, and interferograms of the convolved spectrometer and FPA spectral responses were collected, rather than direct measurements of the convolved spectral responses. This approach has several advantages:

- Unlike a grating monochromator, the FTS has a two-dimensional aperture that is well matched to the FPA and allows a large light throughput,
- Information is collected simultaneously over the entire spectral range of the system,
- Spectral registration is excellent – orders of magnitude better than can be achieved with a grating spectrometer.

This document presents the results of those measurements.



6 Experimental setup

The SLSTR B FPA was installed in the IFS120/5 FTS laboratory at RAL (Figure 6.1) in July 2014 for the spectral calibration of the nine standard FPA channels, S1 – S9. The laboratory was not a clean area, but was cleaned intensively prior to the measurement campaign and was operated under clean room protocols during the campaign. Normal ESD precautions were taken. An earthing point was provided near to the FPA and earth straps were worn whenever in the vicinity of the FPA, or when electrical connections were made to the EGSE.



Figure 6.1 View from the EGSE of the FPA experimental setup in the Brucker IFS 120/5 laboratory. The FTS is immediately behind the EGSE, the FPA in its purged box is to the left of the FTS, the CCA electrical support equipment is in front of the FPA box and the FPA vacuum pump cart is behind.



6.1 FPA

6.1.1 Assembly and integration

The SLSTR Focal Plane Assembly (FPA) and Cryo-Cooler Assembly (CCA) were integrated onto a Ground Support Equipment (GSE) bracket and enclosed in a portable cleanroom box purged with certificated high purity air. The mechanical interface to the spectrometer consisted of vacuum bellows, a ZnSe vacuum window to isolate the FPA and FTS vacuum spaces and a standoff with a vibration damper. The mechanical interface was assembled and mounted onto the FPA under clean room conditions.

6.1.2 Vacuum procedure

The FPA and bellows were operated under vacuum throughout the spectral calibration campaign. The FPA and bellows shared a common vacuum space, separated by a 2.62 mm × 1.61 mm aperture that acted as a restriction. The bellows and FPA had separate vacuum ports connected to a single vacuum pump. The pressure at each port was monitored.

6.1.3 Cooling procedure

The FPA was cooled with the CCA following test procedures defined by Selex Galileo (SG).

The spectral calibration of the FPA was performed at different set point temperatures. The primary calibration was made at a flight-representative temperature of 87K. Additional tests were performed at non-standard temperatures to characterise the thermal sensitivities of the spectral response profiles.

6.1.4 EGSE

The FPA was operated from the FPA Electrical Ground Support Equipment (EGSE) console following test procedures recommended by SG. Channels S4 – S9 were only powered and when the FPA was cooled. Channels S1 – S3 were operated at both ambient and cryogenic temperatures.

The EGSE also provided buffered analogue outputs from detector 1 in each channel and was used to log the entire digital output of the FPA during measurement runs.

6.2 FTS

6.2.1 FTS final optics

The layout of the IFS 120/5 optics compartment was modified significantly to improve the uniformity of the optical beam and to match the beam to the FPA (Figure 6.2). The central part of the collimated beam from the spectrometer, where it is most uniform, was selected by an iris, then expanded by a pair of paraboloid mirrors and directed by a series of relay mirrors to a final, steerable paraboloid mirror which was focused at the FPA pupil. An additional iris at the aperture plane between the two beam expanding paraboloids gave control over the final beam intensity.

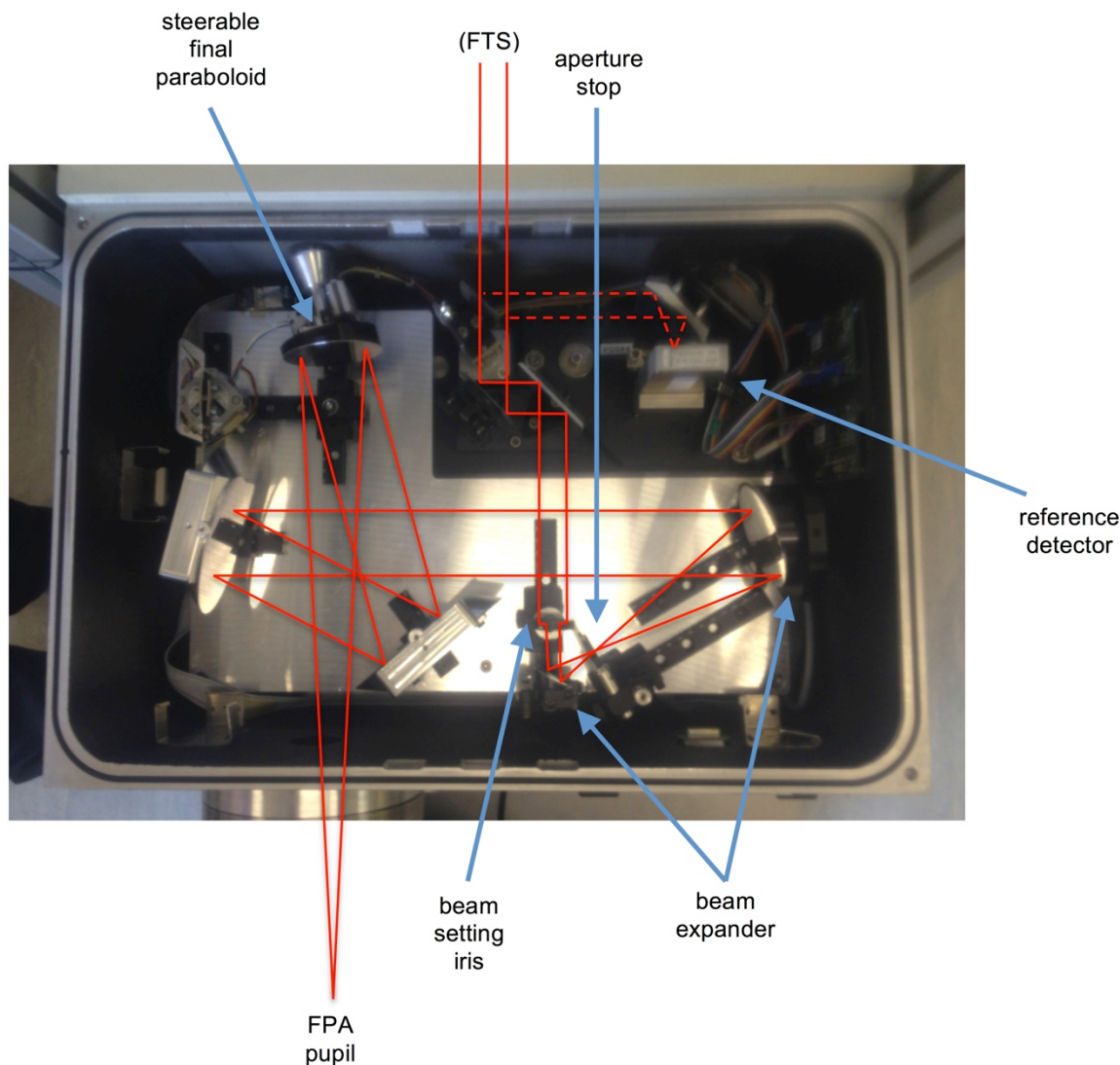


Figure 6.2 Layout of IFS 120/5 optics compartment

6.2.2 FTS operations

FTS operations followed normal practice. The spectrometer was evacuated for all measurements and was operated via the Brucker OPUS interface. Measurement sequences were set up with macro files that contained the required spectrometer settings, including aperture and filter wheel settings, detector source selections and data processing parameters.

6.2.3 FPA analogue measurements

The primary FPA spectral measurements were made with signals from the detector 1 analogue output of the channel under test. The FPA output was coupled to an FTS detector electrical interface with an audio isolating transformer. The FTS detector substituted for a standard FPA detector and the spectrometer recorded a time-resolved interferogram, which was the convolution of the spectrometer's spectral properties, the spectral transmissions of the relay optics and vacuum windows, and the spectral response of the FPA channel itself.



As the FPA analogue output was substituted directly for an FTS detector, the interferogram could be transformed to a spectral response with the spectrometer's standard OPUS processing software.

6.2.4 “Turn-and-turn-about” measurements

A sequence of “turn-and-turn-about” measurements were performed after the completion of the main sequence of FPA measurements, to characterise the relative spectral response of the spectrometer. Once the FPA had been removed from the spectrometer, a small vacuum tank was attached in its place, to house a standard FTS detector mounted at the position of the FPA pupil.

7 Theoretical basis

7.1 FPA spectral response

When the FPA is selected with the FTS flip mirror, the FPA detector records a signal that is a convolution of the spectral intensity of the spectrometer source, the spectral transmission of the spectrometer optics and the spectral response of the selected FPA detector. As the length of the spectrometer arm is changed, a time-resolved interferogram of the convolved spectral response is generated at the detector. The inverse Fourier transform $S_{FPA}(\nu)$ of this interferogram is the convolved spectral response of the optical system:

$$S_{FPA}(\nu) = I_{FTS}(\nu) \tau_{FPA}(\nu) R_{FPA}(\nu) \quad (7.1)$$

where $I_{FTS}(\nu)$ is the spectral intensity at the FTS flip mirror, $\tau_{FPA}(\nu)$ is the spectral transmission from that point to the pupil of the FPA and $R_{FPA}(\nu)$ is the spectral response of the FPA detector, including the internal FPA optical chain.

When the reference detector is selected with the FTS flip mirror, the inverse Fourier transform $S_{ref}(\nu)$ of the interferogram at the reference detector is the convolved spectral response of the new optical system:

$$S_{ref}(\nu) = I_{FTS}(\nu) \tau_{ref}(\nu) R_{ref}(\nu) \quad (7.2)$$

where $I_{FTS}(\nu)$ is again the spectral intensity at the FTS flip mirror, $\tau_{ref}(\nu)$ is the spectral transmission from that point to the reference detector and $R_{ref}(\nu)$ is the spectral response of the reference detector.

Dividing (7.2) by (7.1) and rearranging, the spectral response $R_{FPA}(\nu)$ of the FPA detector is:

$$R_{FPA}(\nu) = [S_{FPA}(\nu)/S_{ref}(\nu)] [\tau_{ref}(\nu)/\tau_{FPA}(\nu)] R_{ref}(\nu) \quad (7.3)$$

$R_{FPA}(\nu)$ is no longer sensitive to the spectral properties of the spectrometer and is a function only of the ratio of two measured quantities $S_{FPA}(\nu)/S_{ref}(\nu)$, the relative spectral transmission of the two optical paths $\tau_{ref}(\nu)/\tau_{FPA}(\nu)$ and the spectral response $R_{ref}(\nu)$ of the reference detector. Writing $T_{rel}(\nu) = \tau_{ref}(\nu)/\tau_{FPA}(\nu)$, the spectral response is:

$$R_{FPA}(\nu) = [S_{FPA}(\nu)/S_{ref}(\nu)] T_{rel} R_{ref}(\nu) \quad (7.4)$$

7.2 Uncertainties in FPA spectral response

Dropping explicit dependences on ν for clarity, then for small uncertainties ΔS_{FPA} , ΔS_{ref} , ΔT_{rel} and ΔR_{ref} in S_{FPA} , S_{ref} , T_{rel} and R_{ref} respectively, the uncertainty ΔR_{FPA} in the FPA spectral response R_{FPA} is:

$$\Delta R_{FPA} = \frac{\partial R_{FPA}}{\partial S_{FPA}} \Delta S_{FPA} + \frac{\partial R_{FPA}}{\partial S_{ref}} \Delta S_{ref} + \frac{\partial R_{FPA}}{\partial T_{rel}} \Delta T_{rel} + \frac{\partial R_{FPA}}{\partial R_{ref}} \Delta R_{ref} \quad (7.5)$$

Solving and rearranging:

$$\frac{\Delta R_{FPA}}{R_{FPA}} = \frac{\Delta S_{FPA}}{S_{FPA}} - \frac{\Delta S_{ref}}{S_{ref}} + \frac{\Delta T_{rel}}{T_{rel}} + \frac{\Delta R_{ref}}{R_{ref}} \quad (7.6)$$

If the uncertainties are uncorrelated, then the terms can be combined in quadrature to generate an estimate:

$$\frac{\Delta R_{FPA}}{R_{FPA}}^2 = \frac{\Delta S_{FPA}}{S_{FPA}}^2 + \frac{\Delta S_{ref}}{S_{ref}}^2 + \frac{\Delta T_{rel}}{T_{rel}}^2 + \frac{\Delta R_{ref}}{R_{ref}}^2 \quad (7.7)$$

7.3 Additional optical elements

If additional optical elements are included in the optical chain to the FPA pupil that are not included either in the reference detector measurements or in the relative transmission measurements, for instance neutral density filters or vacuum windows, then the spectral response $R_{FPA}(\nu)$ defined in (7.4) is a composite of the true FPA spectral response $R_{FPA}^*(\nu)$ and the spectral transmissions $\tau_i(\nu)$ of the n additional optical elements:

$$R_{FPA}(\nu) = R_{FPA}^*(\nu) \prod_{i=1}^n \tau_i(\nu) \quad (7.8)$$

Rearranging, the true FPA spectral response is:

$$R_{FPA}^*(\nu) = R_{FPA}(\nu) \div \prod_{i=1}^n \tau_i(\nu) \quad (7.9)$$

Clearly, in the case where there are no additional optical elements ($n = 0$), $R_{FPA}(\nu)$ and $R_{FPA}^*(\nu)$ are identical.

7.4 Uncertainties due to additional optical elements

Dropping explicit dependences on ν for clarity, then for small uncertainties ΔR_{FPA} and $\Delta \tau_i$ in R_{FPA} and τ_i respectively, the uncertainty ΔR_{FPA}^* in the true FTS spectral response R_{FPA}^* is:

$$\Delta R_{FPA}^* = \frac{\partial R_{FPA}^*}{\partial R_{FPA}} \Delta R_{FPA} + \sum_{i=1}^n \frac{\partial R_{FPA}^*}{\partial \tau_i} \Delta \tau_i \quad (7.10)$$

Solving and rearranging:

$$\frac{\Delta R_{FPA}^*}{R_{FPA}^*} = \frac{\Delta R_{FPA}}{R_{FPA}} - \sum_{i=1}^n \frac{\Delta \tau_i}{\tau_i} \quad (7.11)$$

If the uncertainties are uncorrelated, then the terms can be combined in quadrature to generate an estimate:

$$\frac{\Delta R_{FPA}^*}{R_{FPA}^*} = \frac{\Delta R_{FPA}}{R_{FPA}} + \sum_{i=1}^n \frac{\Delta \tau_i}{\tau_i} \quad (7.12)$$

Again, when there are no additional optical elements ($n = 0$), $\Delta R_{FPA}(\nu)$ and $\Delta R_{FPA}^*(\nu)$ are identical.

7.5 FTS relative spectral transmission

The relative spectral transmission $T_{rel}(\nu)$ of the two FTS optical paths in (7.4) can be determined independently of the FPA measurements with two interchangeable detectors, A and B, installed at the FPA pupil and reference detector positions. The inverse Fourier transforms $S_{A,FPA}(\nu)$ and $S_{B,ref}(\nu)$ of the signals recorded by detector A in the FPA pupil position and detector B in the reference detector position are:

$$S_{A,FPA}(\nu) = I_{FTS}(\nu) \tau_{FPA}(\nu) R_A(\nu) \quad (7.13)$$

$$S_{B,ref}(\nu) = I_{FTS}(\nu) \tau_{ref}(\nu) R_B(\nu) \quad (7.14)$$

where $R_A(\nu)$ and $R_B(\nu)$ are the spectral responses of detectors A and B. Dividing (7.14) by (7.13) and rearranging, the relative spectral transmission is:

$$\tau_{ref}(\nu) / \tau_{FPA}(\nu) = [S_{B,ref}(\nu) / S_{A,FPA}(\nu)] [R_A(\nu) / R_B(\nu)] \quad (7.15)$$

Swapping the detectors and repeating the measurements, the inverse Fourier transforms of the signals recorded by the detectors are:

$$S_{B,FPA}(\nu) = I_{FTS}(\nu) \tau_{FPA}(\nu) R_B(\nu) \quad (7.16)$$

$$S_{A,ref}(\nu) = I_{FTS}(\nu) \tau_{ref}(\nu) R_A(\nu) \quad (7.17)$$

Dividing (7.17) by (7.16) and rearranging, the relative spectral transmission is now:

$$\tau_{ref}(\nu)/\tau_{FPA}(\nu) = [S_{A, ref}(\nu)/S_{B, FPA}(\nu)][R_B(\nu)/R_A(\nu)] \quad (7.18)$$

Finally, multiplying the left and right sides of equations (7.15) and (7.18) and taking the square roots:

$$\tau_{ref}(\nu)/\tau_{FPA}(\nu) = T_{rel}(\nu) = \left[\frac{S_{A, ref}(\nu) S_{B, ref}(\nu)}{S_{A, FPA}(\nu) S_{B, FPA}(\nu)} \right]^{1/2} \quad (7.19)$$

The relative spectral transmission is now a function of four measurements only and is not dependent either on the detector spectral responses or on the spectral properties of the spectrometer.

7.6 Uncertainties in FTS relative spectral transmission

Dropping explicit dependences on ν for clarity, then for small uncertainties $\Delta S_{A, ref}$, $\Delta S_{B, ref}$, $\Delta S_{A, FPA}$ and $\Delta S_{B, FPA}$ in $S_{A, ref}$, $S_{B, ref}$, $S_{A, FPA}$ and $S_{B, FPA}$ respectively, the uncertainty ΔT_{rel} in the FTS relative spectral transmission T_{rel} is:

$$\Delta T_{rel} = \frac{\partial T_{rel}}{\partial S_{A, ref}} \Delta S_{A, ref} + \frac{\partial T_{rel}}{\partial S_{B, ref}} \Delta S_{B, ref} + \frac{\partial T_{rel}}{\partial S_{A, FPA}} \Delta S_{A, FPA} + \frac{\partial T_{rel}}{\partial S_{B, FPA}} \Delta S_{B, FPA} \quad (7.20)$$

Solving and rearranging:

$$\frac{\Delta T_{rel}}{T_{rel}} = \frac{1}{2} \left(\frac{\Delta S_{A, ref}}{S_{A, ref}} + \frac{\Delta S_{B, ref}}{S_{B, ref}} - \frac{\Delta S_{A, FPA}}{S_{A, FPA}} - \frac{\Delta S_{B, FPA}}{S_{B, FPA}} \right) \quad (7.21)$$

If the uncertainties are uncorrelated, then the terms can be combined in quadrature to generate an estimate:

$$\frac{\Delta T_{rel}}{T_{rel}}^2 = \frac{1}{4} \left(\frac{\Delta S_{A, ref}^2}{S_{A, ref}^2} + \frac{\Delta S_{B, ref}^2}{S_{B, ref}^2} + \frac{\Delta S_{A, FPA}^2}{S_{A, FPA}^2} + \frac{\Delta S_{B, FPA}^2}{S_{B, FPA}^2} \right) \quad (7.22)$$

7.7 Spectral transmission of an optical element

The spectral transmission of an individual optical element, such as a filter or a window, can be determined with a single detector independently of the FPA measurements. When the element is installed between the spectrometer and the detector, the inverse Fourier transform $S_i(\nu)$ of the interferogram recorded by the detector is:

$$S_i(\nu) = I_{FTS}(\nu) \tau_i(\nu) R(\nu) \quad (7.23)$$

where $I_{FTS}(\nu)$ is the spectral intensity illuminating the element, $\tau_i(\nu)$ is the spectral transmission of the element and $R(\nu)$ is the spectral response of the detector. With the element removed, the inverse Fourier transform $S_0(\nu)$ of the interferogram at the detector is the convolved spectral response of the remaining optical system:

$$S_0(\nu) = I_{FTS}(\nu) R(\nu) \quad (7.24)$$

Taking the ratio of (7.23) and (7.24) and rearranging, the spectral transmission of the element is:

$$\tau_i(\nu) = S_i(\nu)/S_0(\nu) \quad (7.25)$$

7.8 Uncertainties in the spectral transmission of an optical element

Dropping explicit dependences on ν for clarity, then for small uncertainties ΔS_i and ΔS_0 in S_i and S_0 respectively, the uncertainty $\Delta \tau_i$ in the spectral transmission τ_i is:

$$\Delta \tau_i = \frac{\partial \tau_i}{\partial S_i} \Delta S_i + \frac{\partial \tau_i}{\partial S_0} \Delta S_0 \quad (7.26)$$

Solving and rearranging:

$$\frac{\Delta \tau_i}{\tau_i} = \frac{\Delta S_i}{S_i} - \frac{\Delta S_0}{S_0} \quad (7.27)$$

If the uncertainties are uncorrelated, then the terms can be combined in quadrature to generate an estimate:

$$\frac{\Delta \tau_i^2}{\tau_i^2} = \frac{\Delta S_i^2}{S_i^2} + \frac{\Delta S_0^2}{S_0^2} \quad (7.28)$$

8 Measurements

8.1 Detector measurements

The relative spectral responsivities of four Brucker FTS detectors were calibrated by the UK National Physical Laboratory (NPL) between the 3rd May and the 4th June 2014 (RD 1, RD 2, RD 3, RD 4). All SLSTR FPA spectral responses are scaled from these measurements (Section 7.1). The data supplied in the calibration certificates are summarised in the following subsections.

8.1.1 Silicon diode detector (Brucker ID510/8, S/N 172)

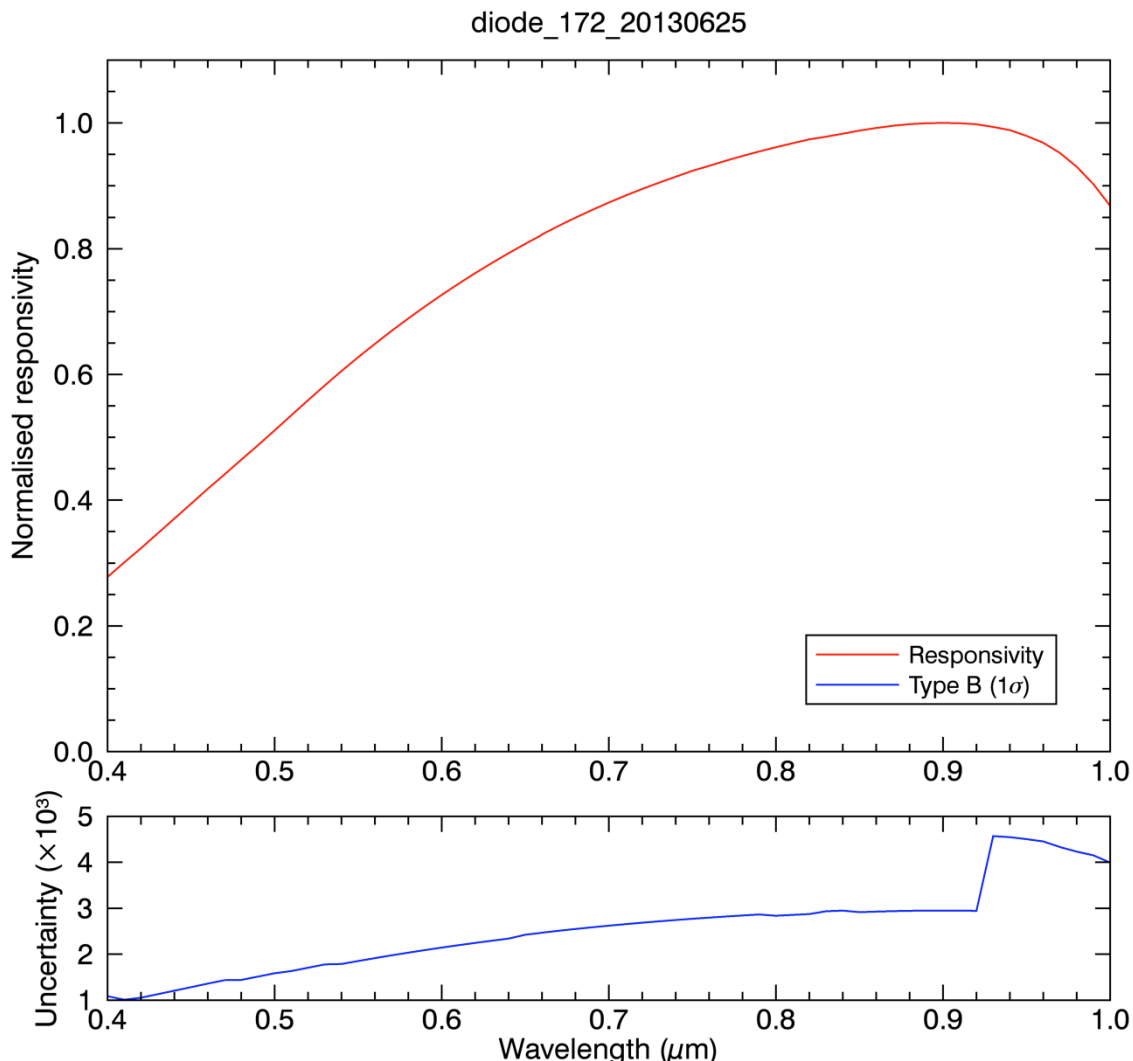


Figure 8.1 The relative spectral responsivity of Brucker ID510/8 silicon diode detector S/N 172.



8.1.2 Silicon diode detector (Brucker ID510/8, S/N 182)

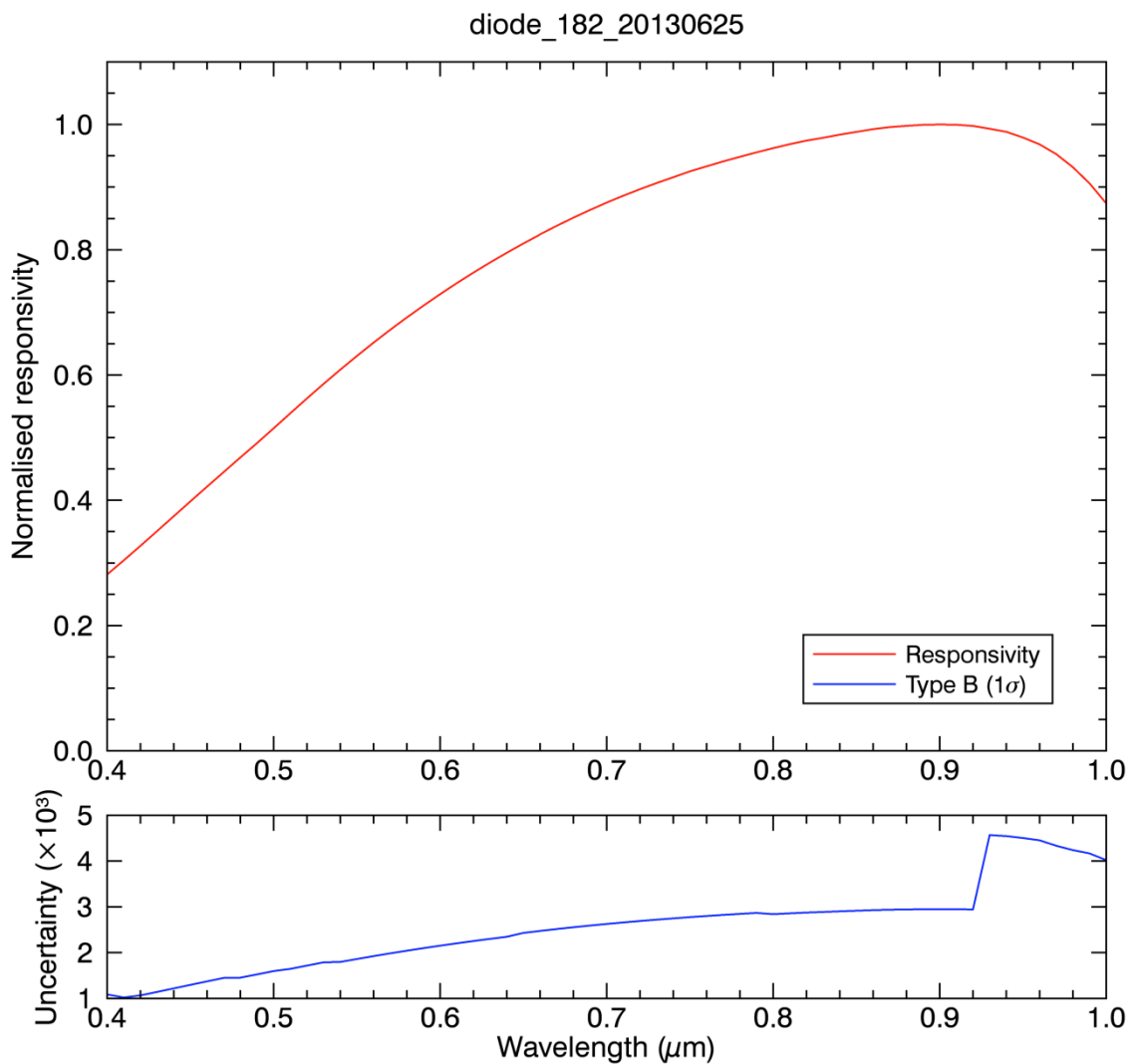


Figure 8.2 The relative spectral responsivity of Brucker ID510/8 silicon diode detector S/N 182.

8.1.3 DLATGS detector (Brucker ID301/8, S/N 7083)

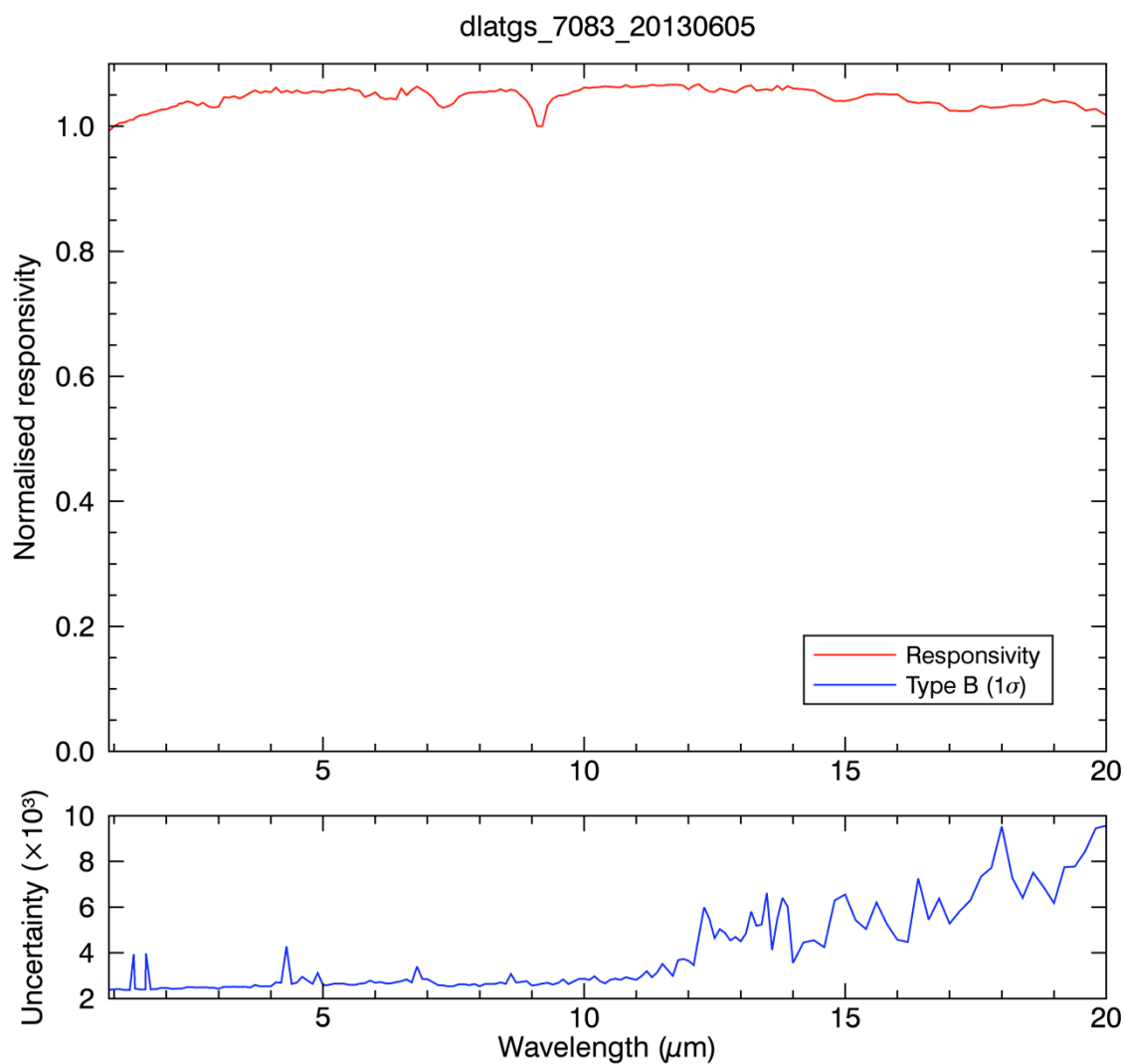


Figure 8.3 The relative spectral responsivity of Brucker ID301/8 DLATGS detector S/N 7083.



8.1.4 DLATGS detector (Brucker ID301/8, S/N 8014)

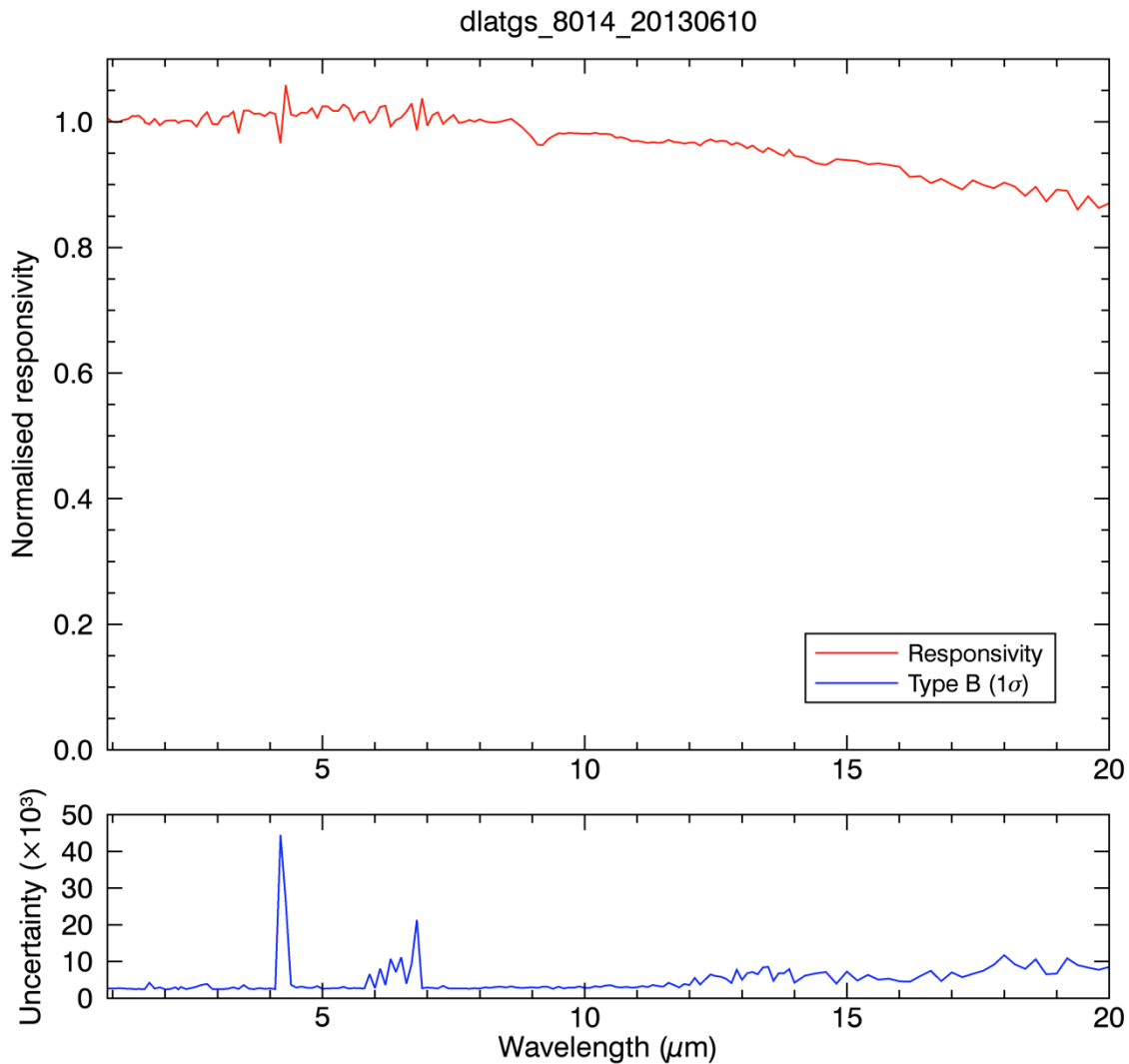


Figure 8.4 The relative spectral responsivity of Brucker ID301/8 DLATGS detector S/N 8014.

8.2 FTS relative spectral transmission

The FTS optical paths to the FPA pupil and the internal FTS reference detector have different spectral transmissions. As measurements of the FPA spectral response are referred to the calibrated FTS reference detector, the FTS measurements are adjusted for the relative spectral transmissions of the two paths (Section 7.1).

The relative transmissions for each of three spectrometer configurations used for the FPA measurements were derived from “turn-and-turn-about” measurement sequences with two optically and mechanically compatible detectors, placed either in the normal reference detector position or substituted for the FPA at the FPA pupil position (Section 7.5). The measurements were made independently of the FPA and included the ZnSe vacuum window in the path to the FPA pupil position. The spectrometer configurations were:

- a) Quartz halogen lamp source, quartz beamsplitter, silicon detectors (S1 – S3),
- b) Quartz halogen lamp source, CaF₂ beamsplitter, DALTGS detectors (S4 – S7),
- c) Globar source, KBr/Ge beamsplitter, DALTGS detectors (S7 – S9).

In each configuration, measurements were made for each of the four permutations of detector and position. The sequence was then repeated in reverse order, so that small drifts could be averaged out.

The FTS relative spectral transmissions derived from the measurements for each of the spectrometer configurations are summarised in the following subsections.



8.2.1 FTS visible relative spectral transmission (S1 – S3)

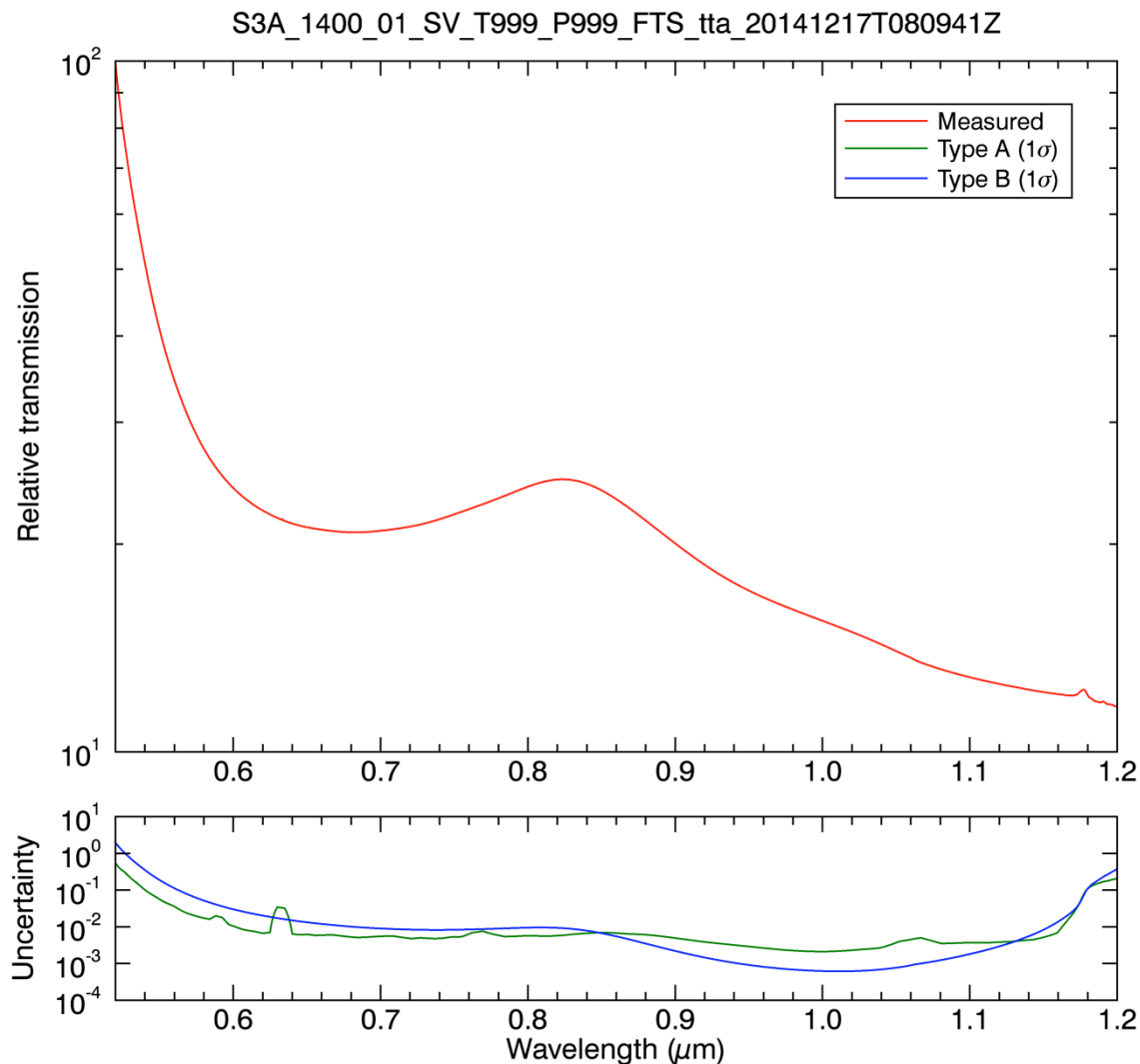


Figure 8.5 FPA SWIR relative spectral transmission for channels S4 – S6 (quartz halogen lamp source, CaF_2 beamsplitter, DALTGS detectors)



8.2.2 FTS SWIR relative transmission (S4 – S7)

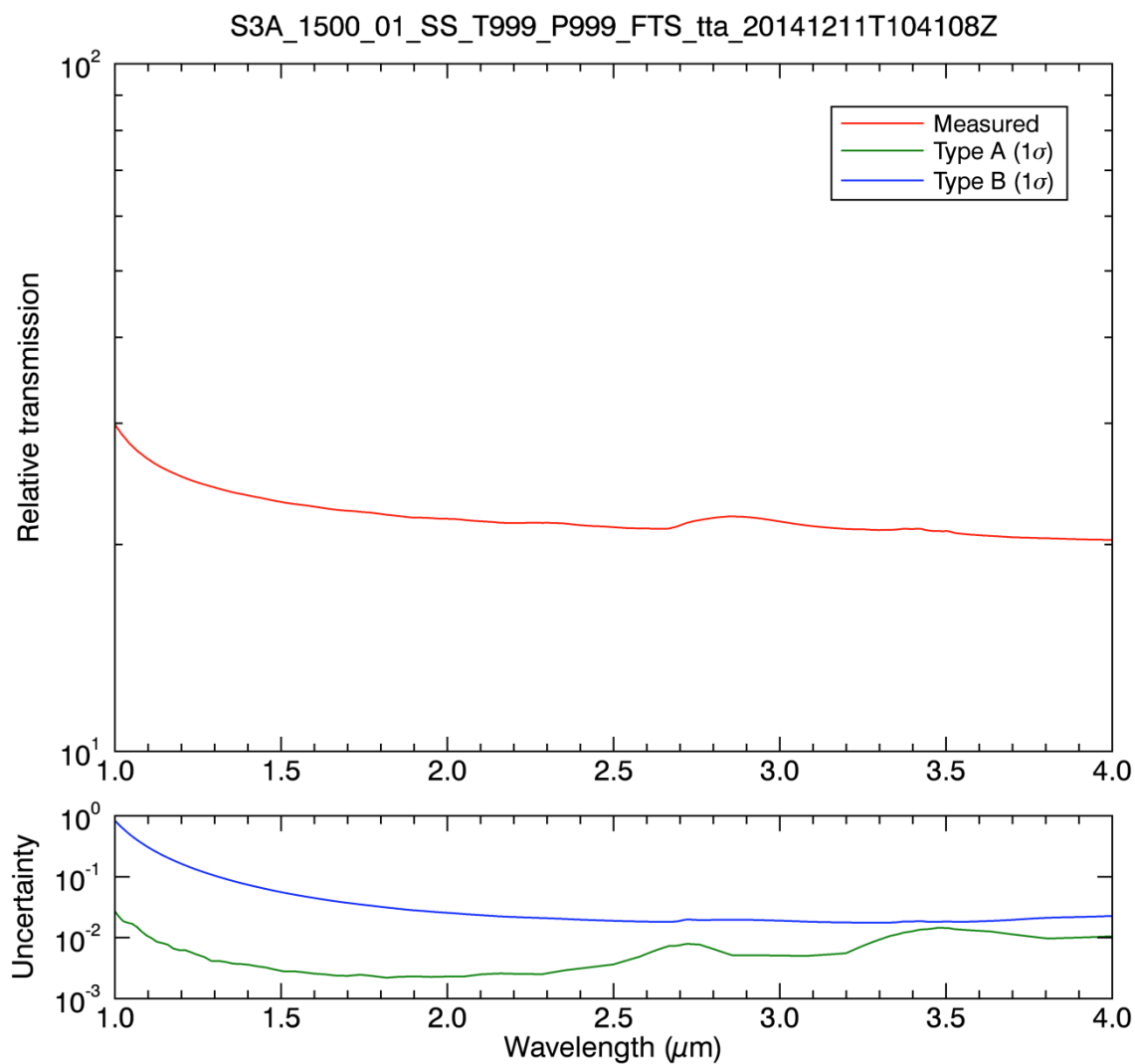


Figure 8.6 FPA visible relative spectral transmission for channels S4 – S6 (quartz halogen lamp source, quartz beamsplitter, silicon detectors)



8.2.3 FTS TIR relative transmission (S7 – S9)

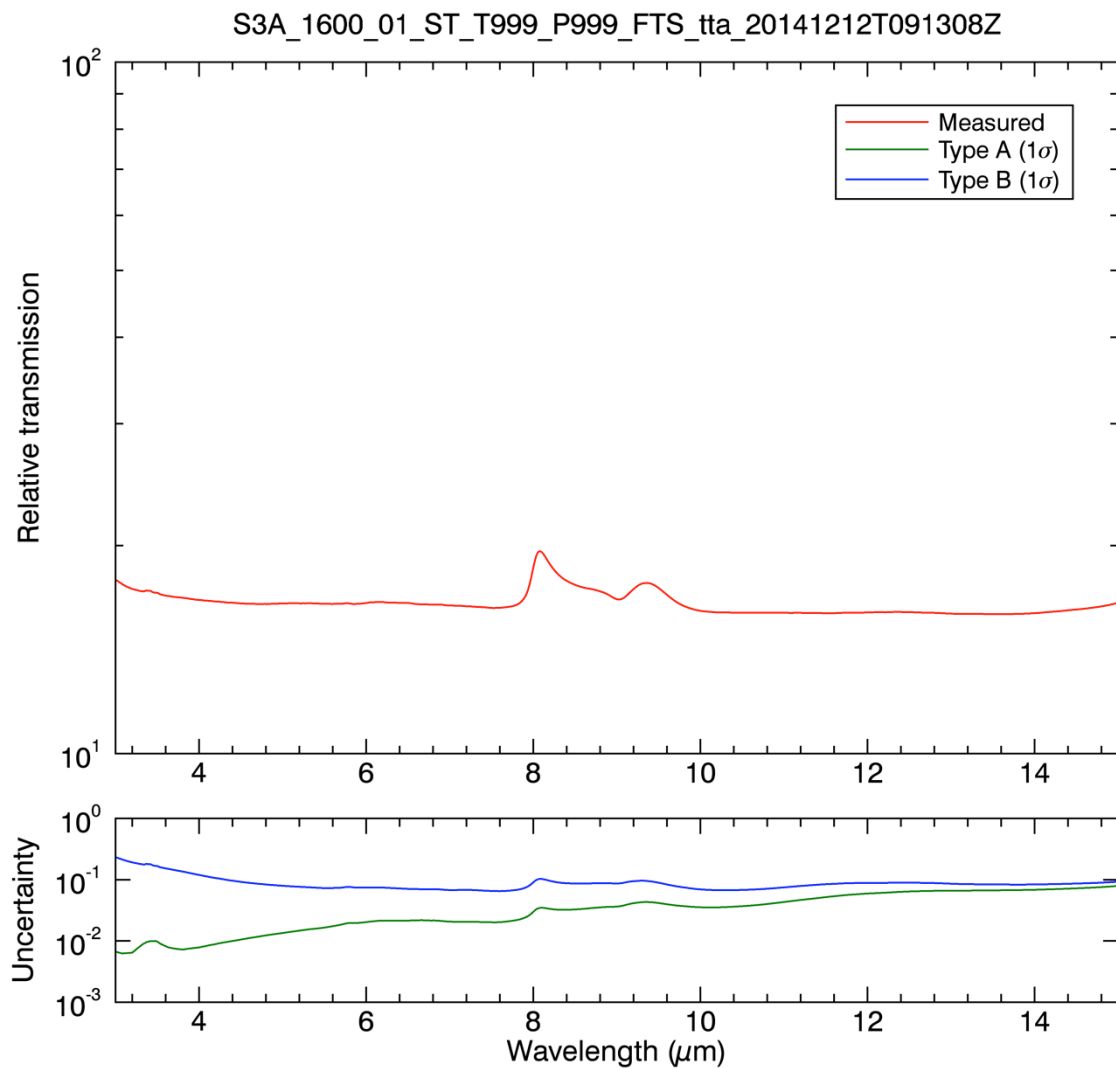


Figure 8.7 FPA TIR relative spectral transmission for channels S7 – S9 (globar source, KBr/Ge beamsplitter, DALTGS detectors)

8.3 Neutral density filters and out-of-band filters

For some FPA characterisation measurements, neutral density filters or out-of-band blocking filters were installed in one or more of three different positions within the IFS 120/5 spectrometer, to match the FTS spectral emission intensity to the dynamic ranges of the FPA and FTS reference detectors. These positions were:

- a) A filter wheel in the common optical path shared by the FPA and reference detectors,
- b) A sample compartment in the common optical path shared by the FPA and reference detectors,
- c) The detector compartment in the optical path of the FPA detectors only.

The spectral transmissions of filters installed in the sample compartment, or in the filter wheel when the same wheel position is used for both FPA and reference detector measurements, cancel from the final calibrated spectral responses of the FPA detectors and do not need to be characterised separately.

The spectral transmissions of filters installed in the detector compartment, or in the filter wheel when different wheel positions are used for FPA and reference measurements, modify the spectral shapes of the FPA detector responses. Filters installed in these positions were characterised individually so that their measured spectral transmissions could be applied to the calibrated FPA detector responses (Section 7.3).

The filters were characterised in the positions where they were used for FPA measurements so that they were measured in an optical beam of the correct speed.

All filter measurement sequences were made up of a symmetric sequence of measurements with the filter installed, interleaved with reference measurements with the filter removed. Each measurement consisted of a number of spectrometer scans, averaged so that the measurement noise was reduced.

The filter spectral transmissions derived from the measurements are summarised in the following subsections.



8.3.1 0.1% SWIR neutral density filter (Thorlabs NENIR30B)

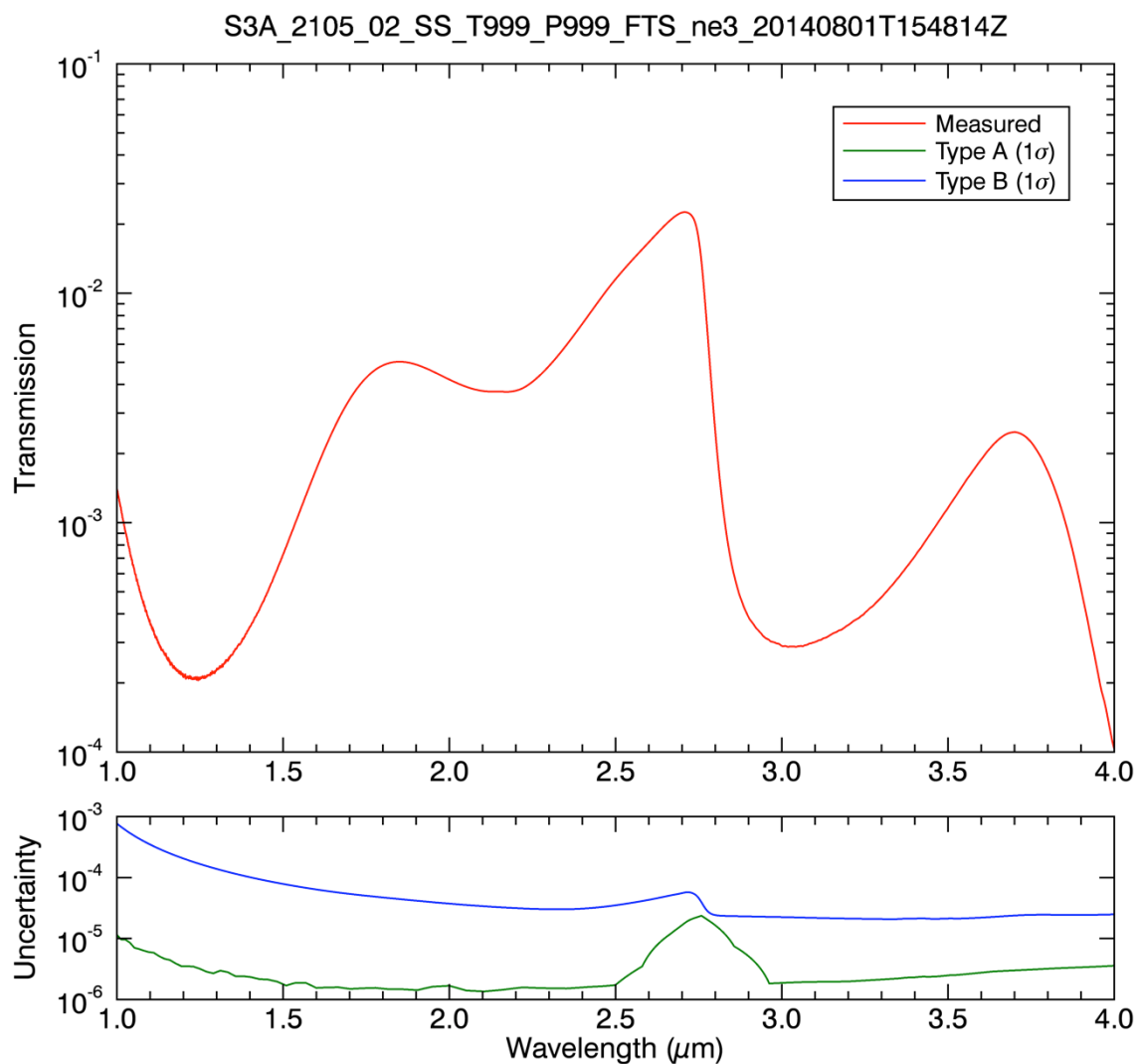


Figure 8.8 The spectral transmission of Thorlabs NENIR30B 0.1% SWIR neutral density filter.



8.3.2 1% SWIR neutral density filter (Thorlabs NENIR20B)

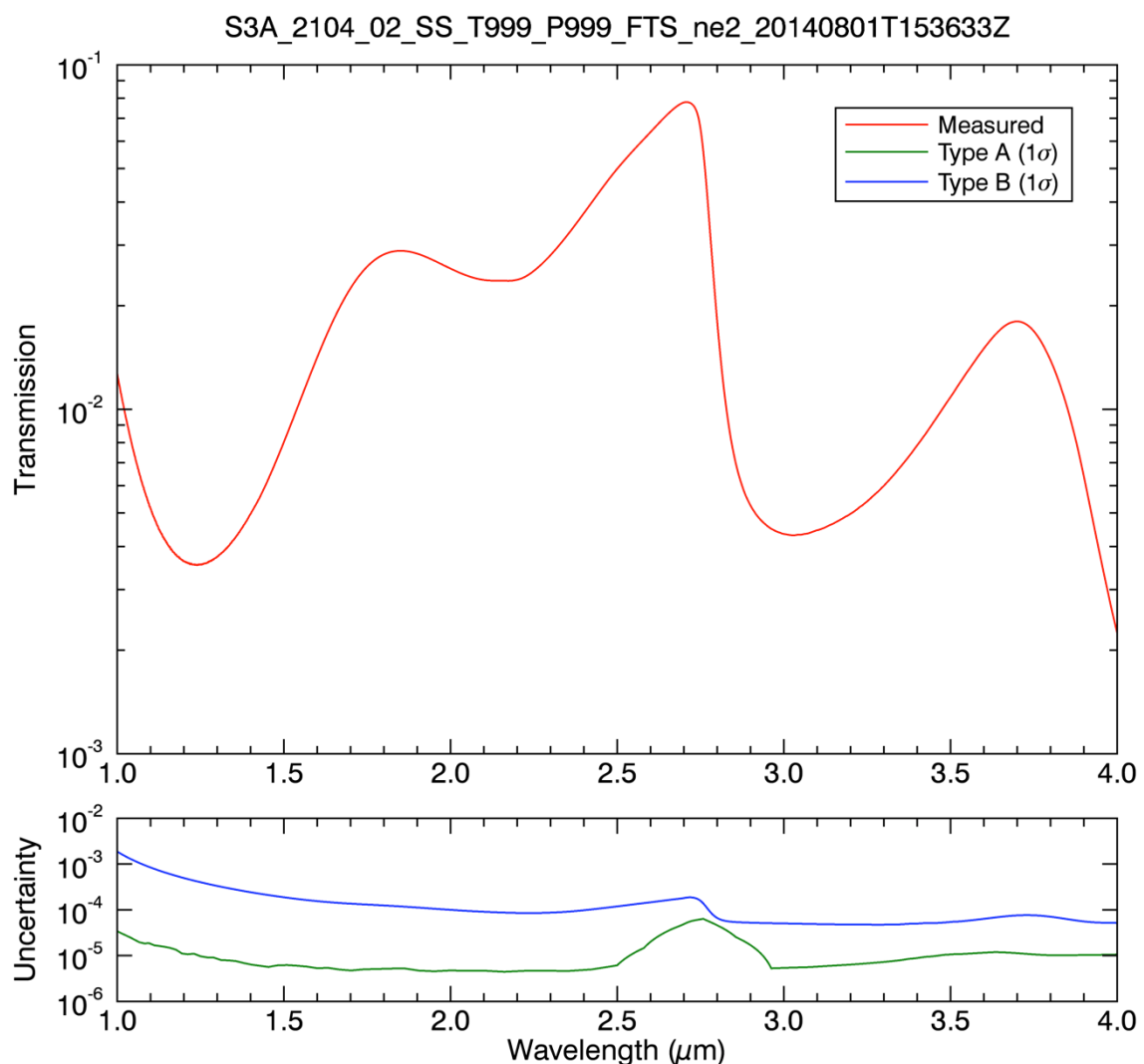


Figure 8.9 The spectral transmission of Thorlabs NENIR20B 1% SWIR neutral density filter.



8.3.3 1% TIR neutral density filter (Thorlabs NDIR20B)

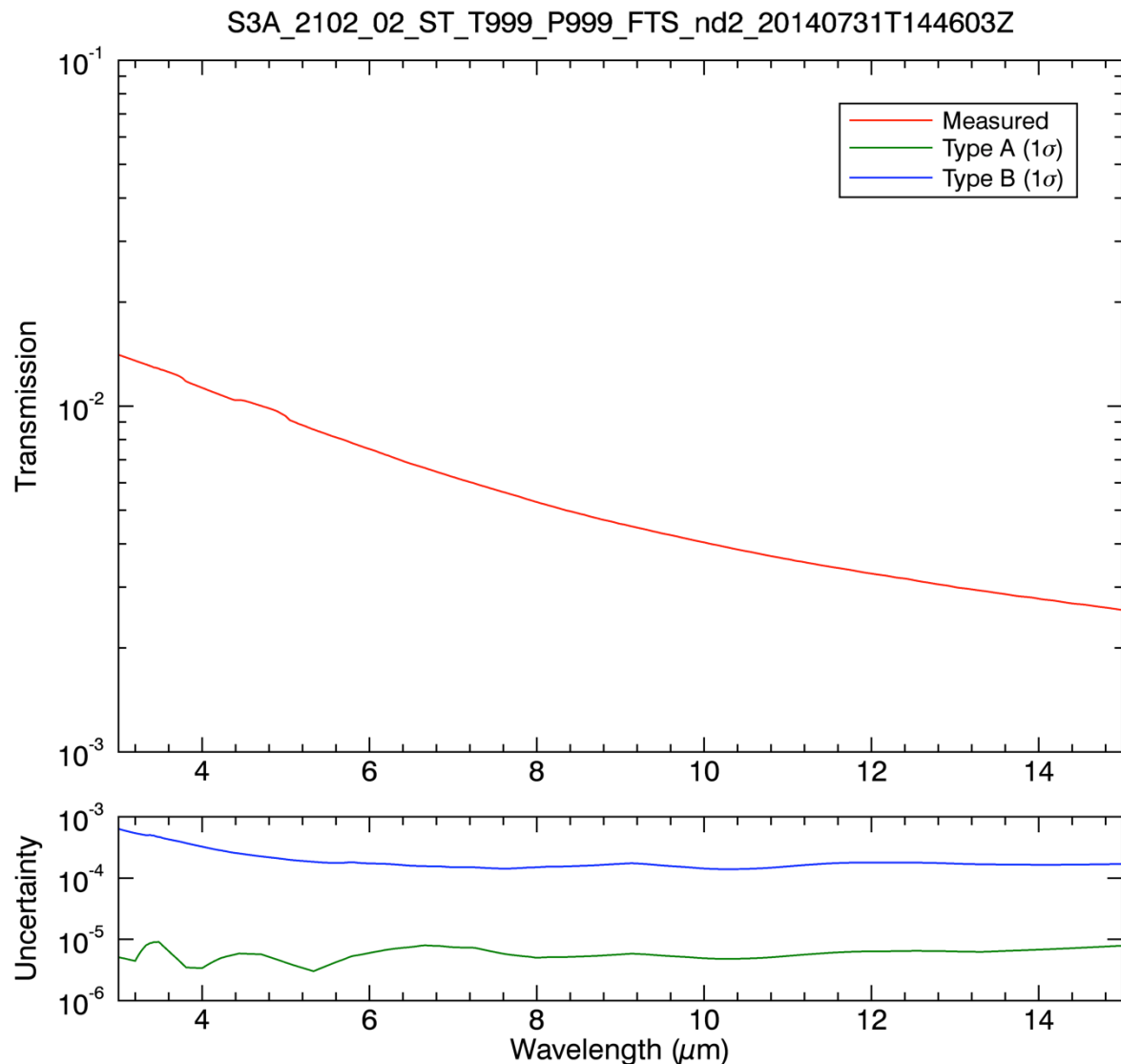


Figure 8.10 The spectral transmission of Thorlabs NDIR20B 1% TIR neutral density filter.

8.4 FPA unpolarised spectral response at 87K

Unpolarised spectral responses generated from the FPA detector 1 analogue outputs at a nominal FPA temperature of 87K are reported in the following subsections. Each subsection contains a graph showing:

- a) The normalised spectral response of the detector derived from spectrometer measurements,
- b) Estimates of type A and type B uncertainties associated with the measurements,
- c) The predicted channel response derived from measurements on individual FPA optical elements.

Each normalised response was derived from the ratio of matched FPA and reference measurements (Section 7.1) scaled by:

- a) The relative spectral response of the optical paths to the FPA and the reference detector,
- b) Where included, the spectral transmissions of any additional optical elements in the optical paths (Section 7.3),
- c) The spectral responsivity of the reference detector.

The detectors in channels S1, S2 and S3 are not cooled, however some of the elements in the detector optical chains are operated at cryogenic temperatures and may have some spectral sensitivity to FPA operating temperature. The mechanical alignment between the cooled and uncooled components is also sensitive to FPA temperature.

Additional neutral density filters were added in the optical path to the FPA for some measurements in order to match more closely the responsivities of the FPA and reference detectors, particularly for channels S4, S5, S6 and S7.

The core FPA measurement sequence consisted of three measurements, taken in quick succession. A background measurement was taken with a calibrated reference detector (Section 8.1), followed by a measurement of the FPA response and then a second measurement with the reference detector. Each measurement consisted of a number of FTS scans, averaged to improve the measurement noise. The two reference measurements were also averaged to reduce the sensitivity to any small drifts over the measurement sequence.

Type A uncertainties were derived from the standard deviations of small measurement bins, covering overlapping wavenumber intervals. Raw measurements were differenced against a Gaussian filtered version of the same data and the resulting standard deviations were adjusted to match the standard deviations of the raw data alone in intervals where there was little or no spectral signal. This is, in effect, a high pass filter that reduces the sensitivity of the uncertainty estimate to the gross filter shape.

Type B uncertainties were estimated from linear interpolations in wavenumber between response minima in the raw FTS spectra, on the presumption that these were (generous) estimates of the position of the spectrum baseline position, and from uncertainty estimates provided with the reference detector calibrations. Other possible sources of type B uncertainty are not yet included, due to the difficulty of assigning realistic values.

The results are presented in the following subsections. Each subsection summarises one channel and contains two figures:

- a) A plot summarising the SRD response template, the normalised spectral responsivity of the channel derived from measurements on individual elements, the measured responsivity of detector 1 and estimates of the type A and type B uncertainties associated with the measurement,
- b) A schematic diagram of the spectrometer setups for the FTS and reference detector measurements showing (from left to right) the filters installed in the FTS filter wheel, the FTS sample compartment and (for FPA measurements only) the FTS detector compartment.

8.4.1 S1 unpolarised spectral response (FPA at 87K)

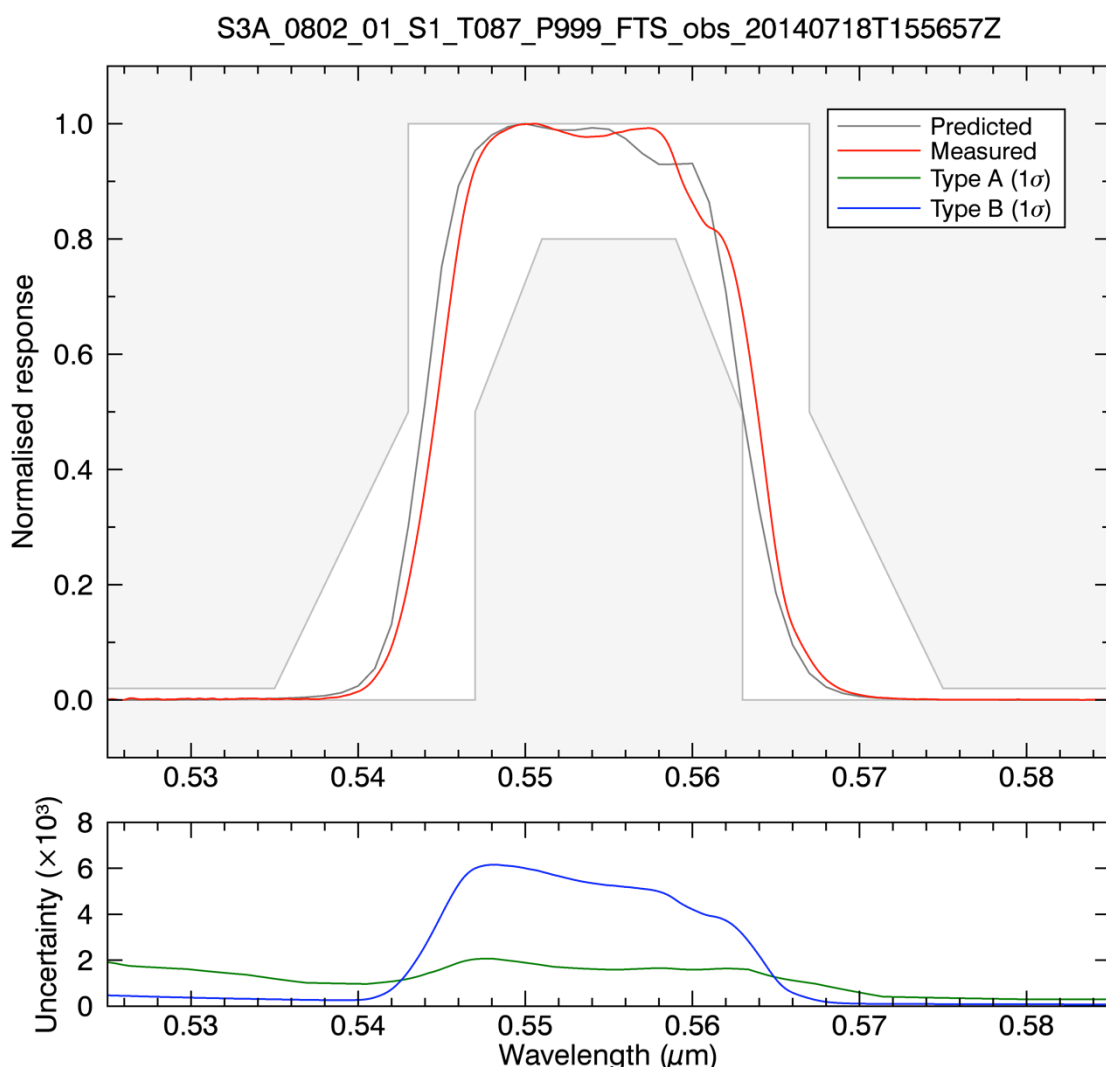


Figure 8.11 The normalised spectral response of S1 detector 1 (analogue signal) at 87K.

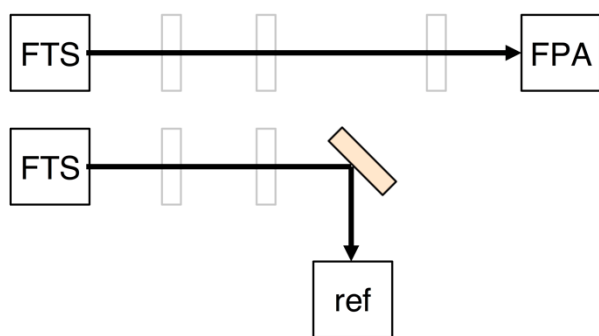


Figure 8.12 Spectrometer schematic setup for S1 FPA and reference measurements. No additional filters were installed.



8.4.2 S2 unpolarised spectral response (FPA at 87K)

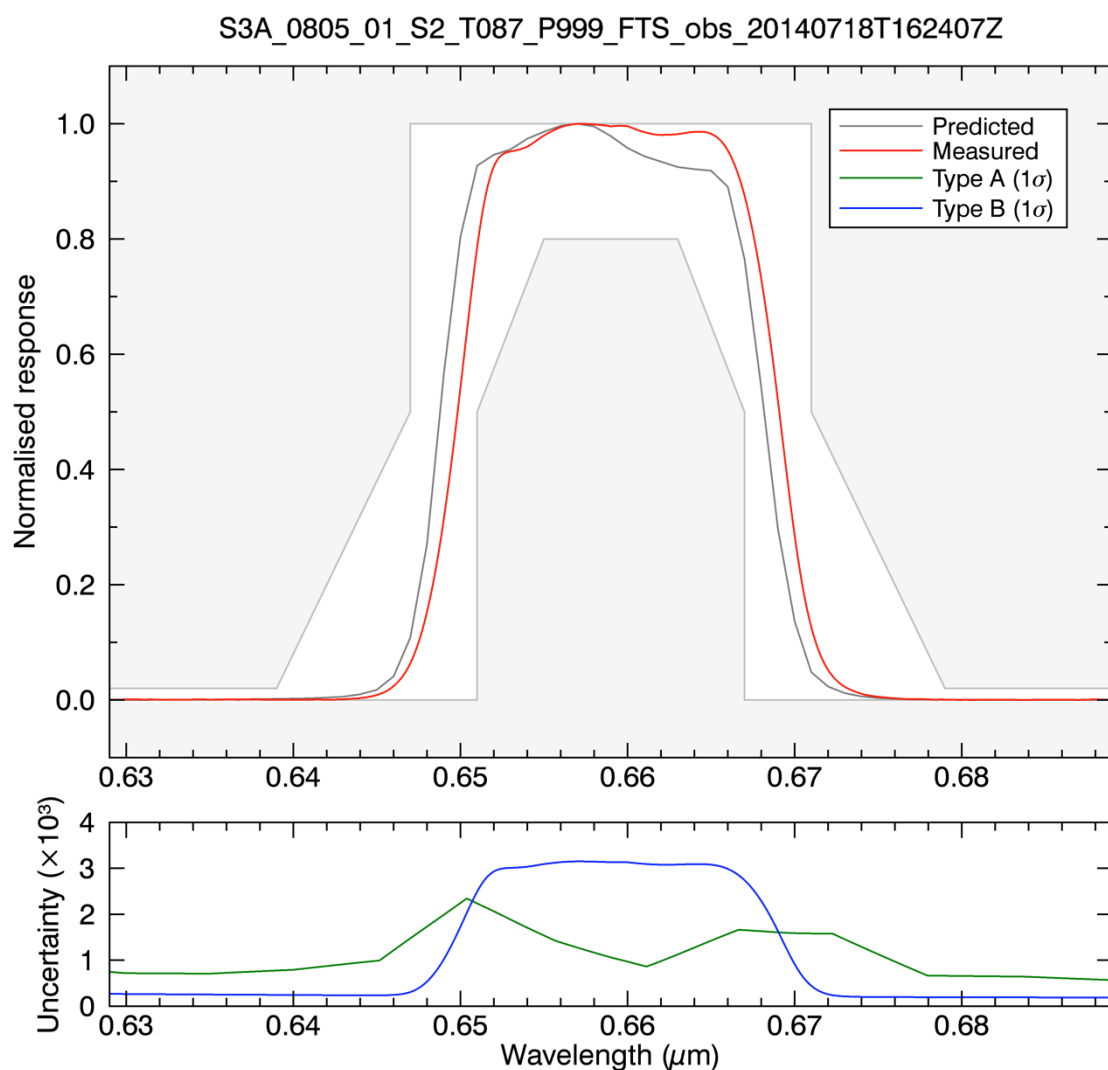


Figure 8.13 The normalised unpolarised spectral response of S2 detector 1 (analogue signal) at 87K.

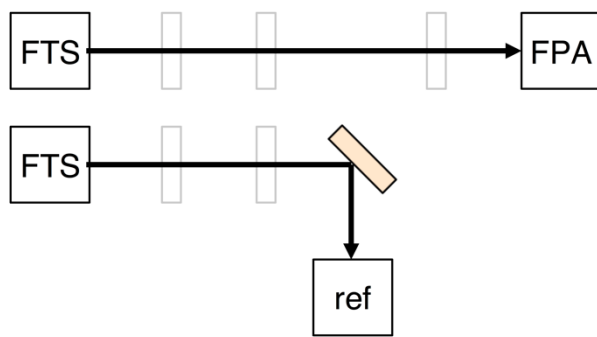


Figure 8.14 Spectrometer schematic setup for S2 FPA and reference measurements. No additional filters were installed.



8.4.3 S3 unpolarised spectral response (FPA at 87K)

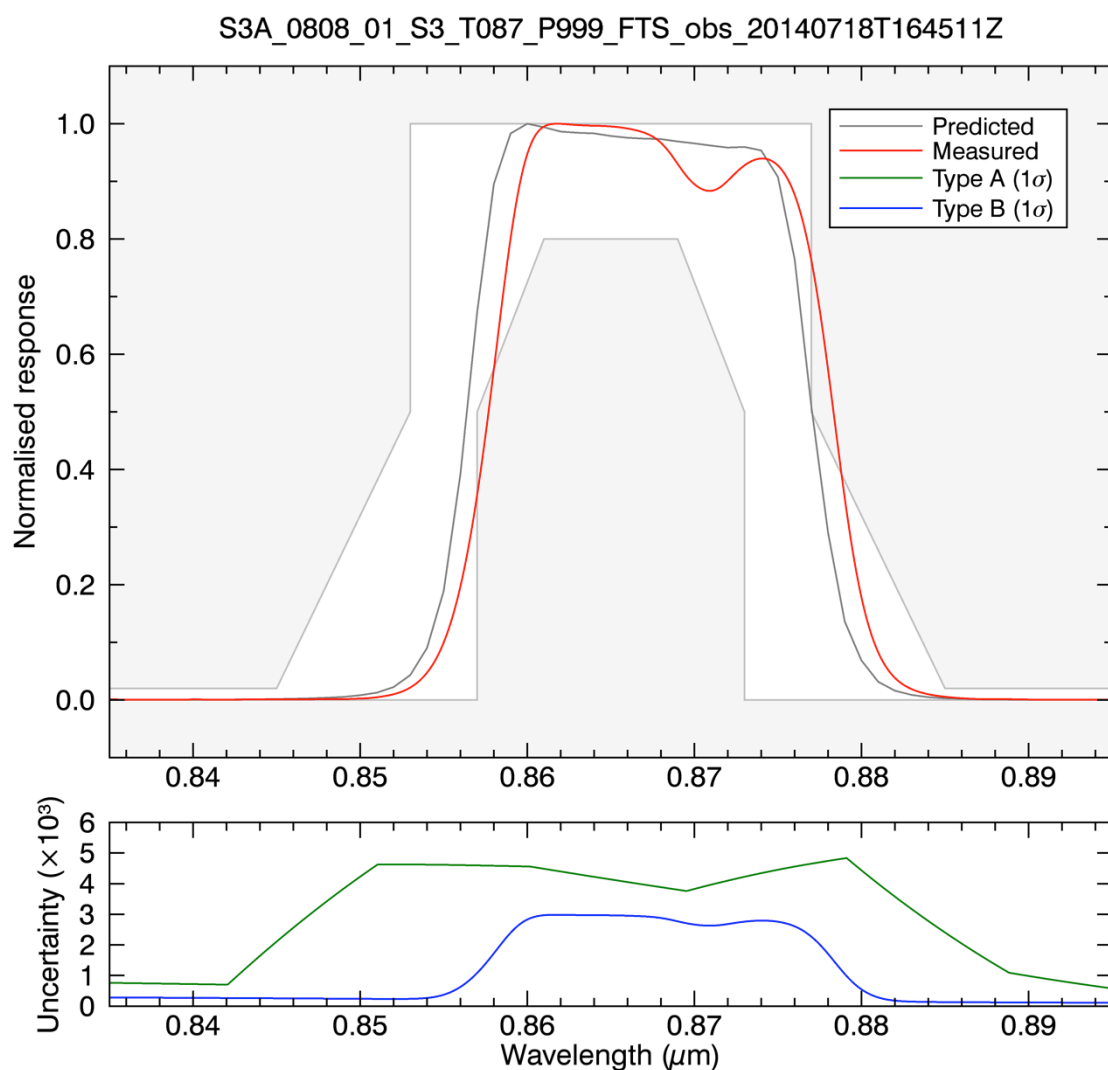


Figure 8.15 The normalised unpolarised spectral response of S3 detector 1 (analogue signal) at 87K.

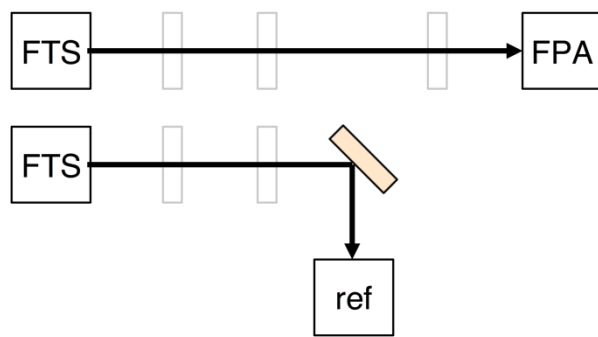


Figure 8.16 Spectrometer schematic setup for S3 FPA and reference measurements. No additional filters were installed.

8.4.4 S4 unpolarised spectral response at 87K

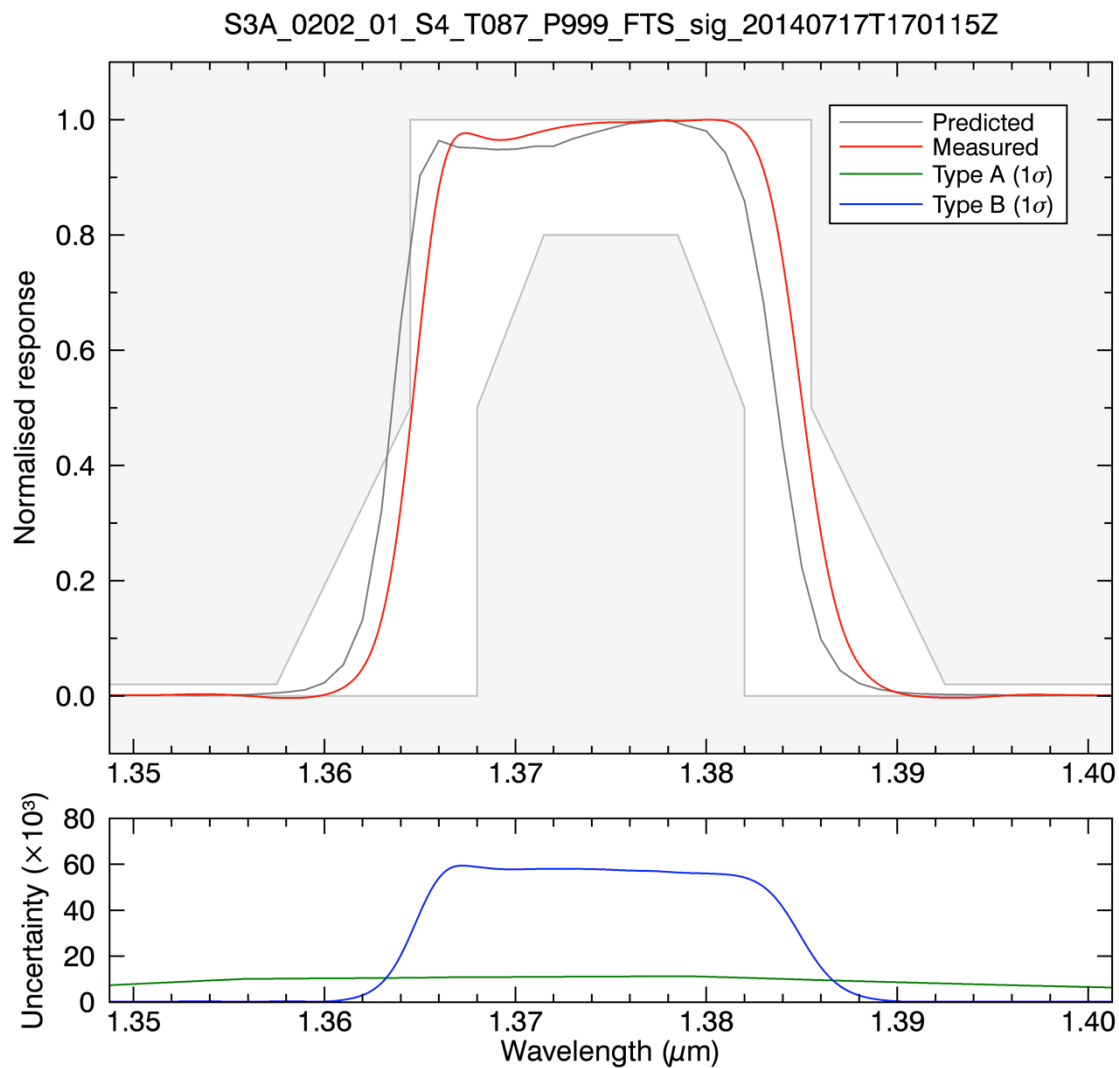


Figure 8.17 The normalised unpolarised spectral response of S4 detector 1 (analogue signal) at 87K.

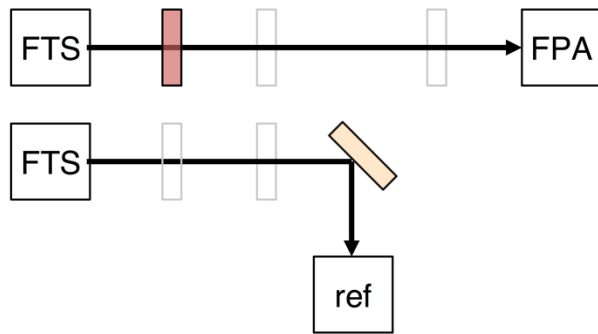


Figure 8.18 Spectrometer schematic setup for S4 FPA and reference measurements. 1% neutral density filter NENIR20B was selected in the filter wheel for the FPA measurement only.

8.4.5 S5 unpolarised spectral response at 87K

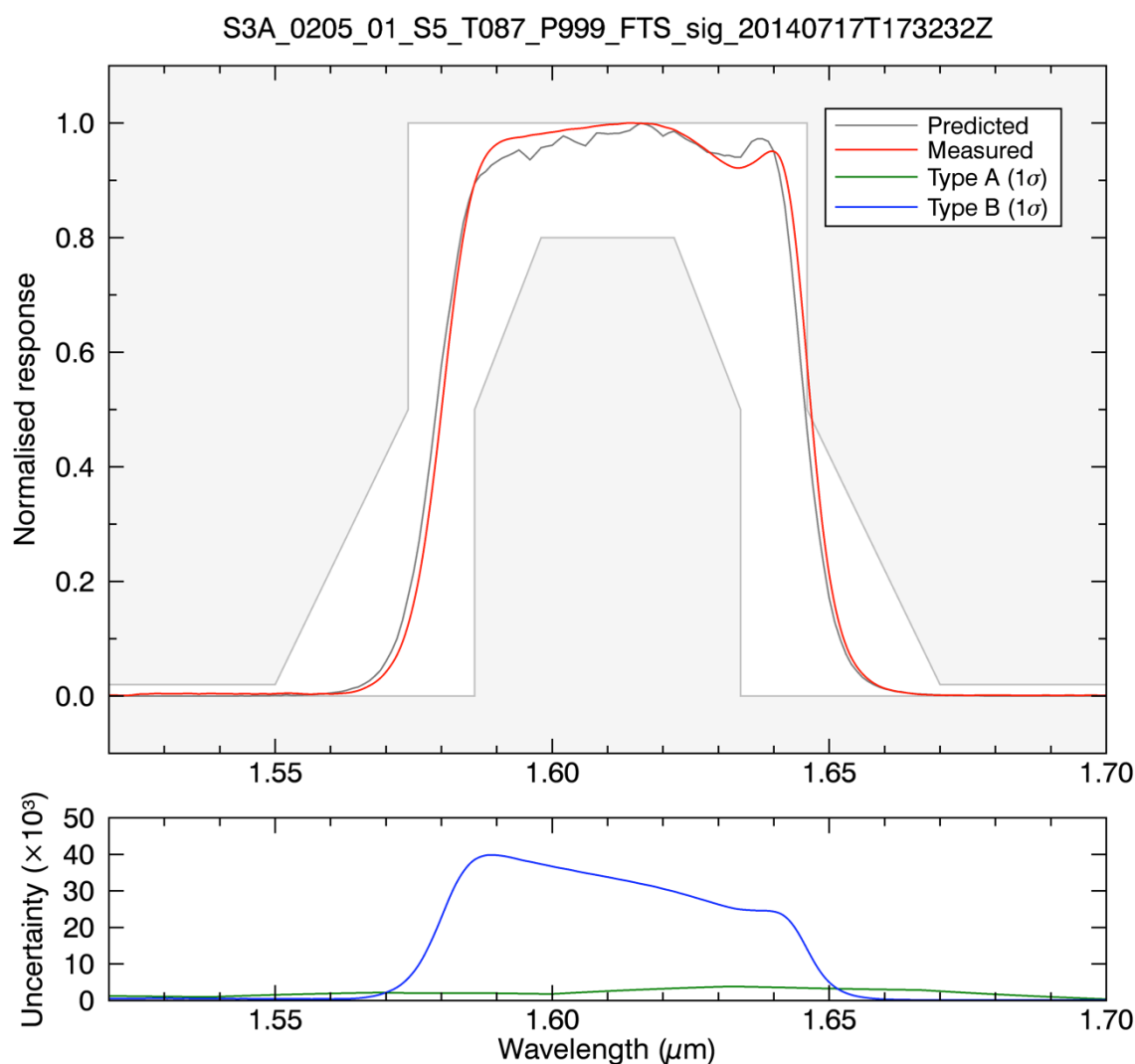


Figure 8.19 The normalised unpolarised spectral response of S5 detector 1 (analogue signal) at 87K.

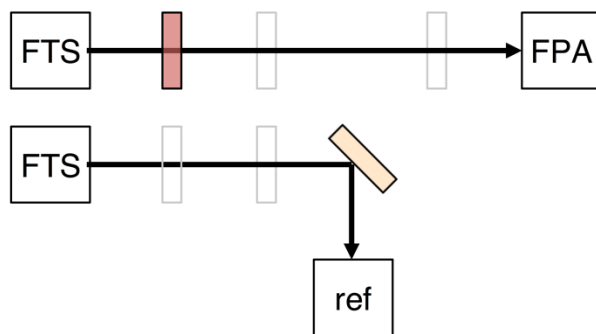


Figure 8.20 Spectrometer schematic setup for S5 FPA and reference measurements. 0.1% neutral density filter NENIR30B was selected in the filter wheel for the FPA measurement only.

8.4.6 S6 unpolarised spectral response at 87K

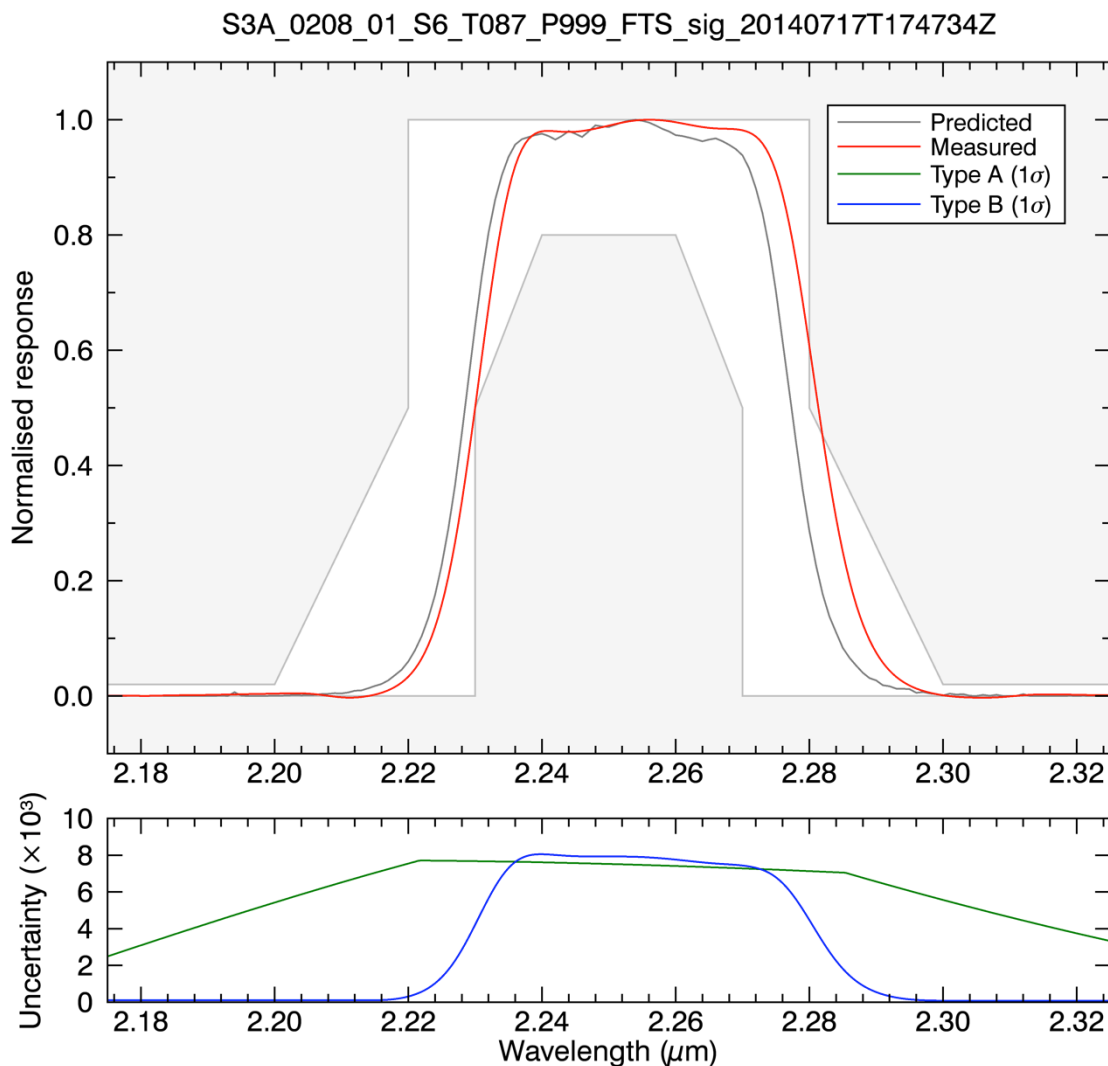


Figure 8.21 The normalised unpolarised spectral response of S6 detector 1 (analogue signal) at 87K.

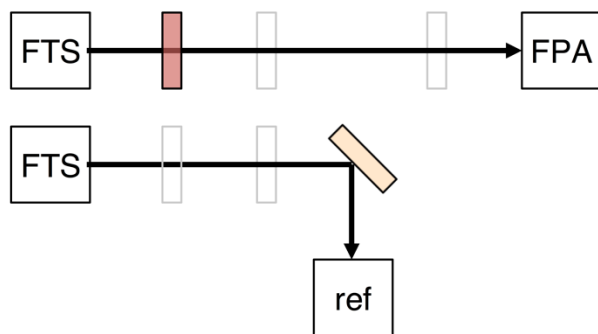


Figure 8.22 Spectrometer schematic setup for S6 FPA and reference measurements. 0.1% neutral density filter NENIR30B was selected in the filter wheel for the FPA measurement only.

8.4.7 S7 unpolarised spectral response at 87K

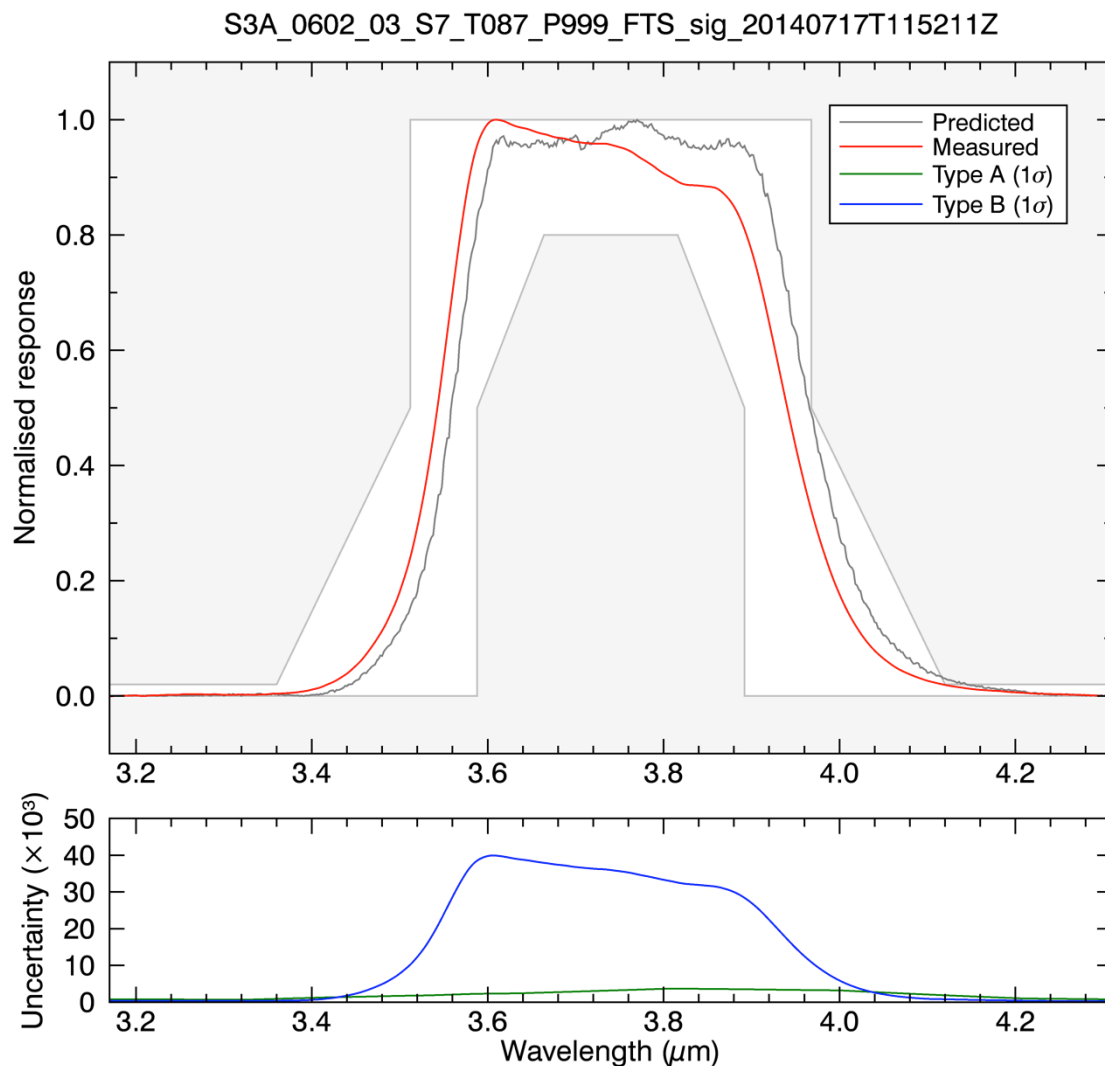


Figure 8.23 The normalised unpolarised spectral response of S7 detector 1 (analogue signal) at 87K.

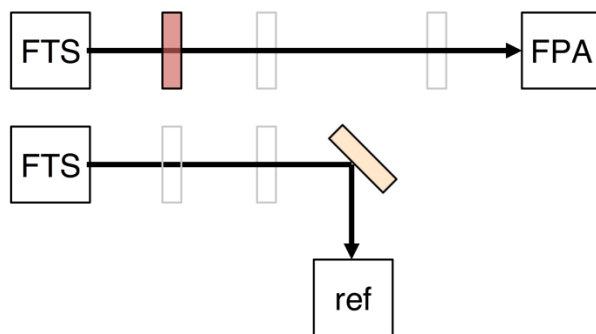


Figure 8.24 Spectrometer schematic setup for S7 FPA and reference measurements. 1% neutral density filter NDIR20B was selected in the filter wheel for the FPA measurement only.

8.4.8 S8 unpolarised spectral response at 87K

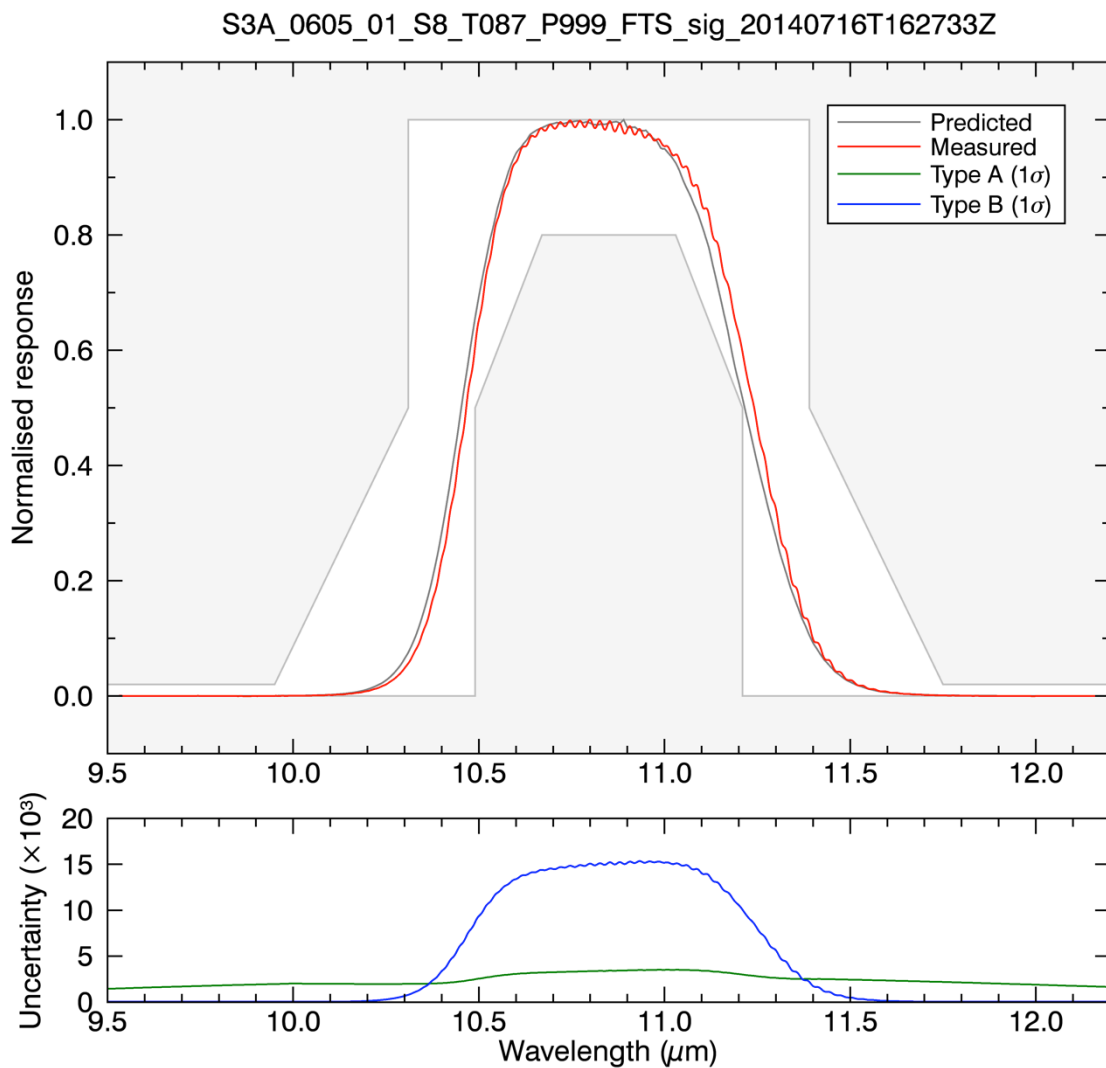


Figure 8.25 The normalised unpolarised spectral response of S8 detector 1 (analogue signal) at 87K.

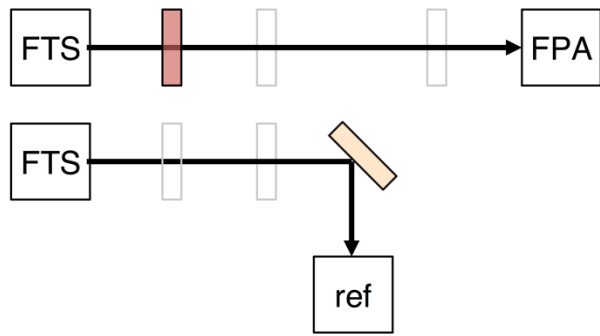


Figure 8.26 Spectrometer schematic setup for S8 FPA and reference measurements. No additional filters were installed.

8.4.9 S9 unpolarised spectral response at 87K

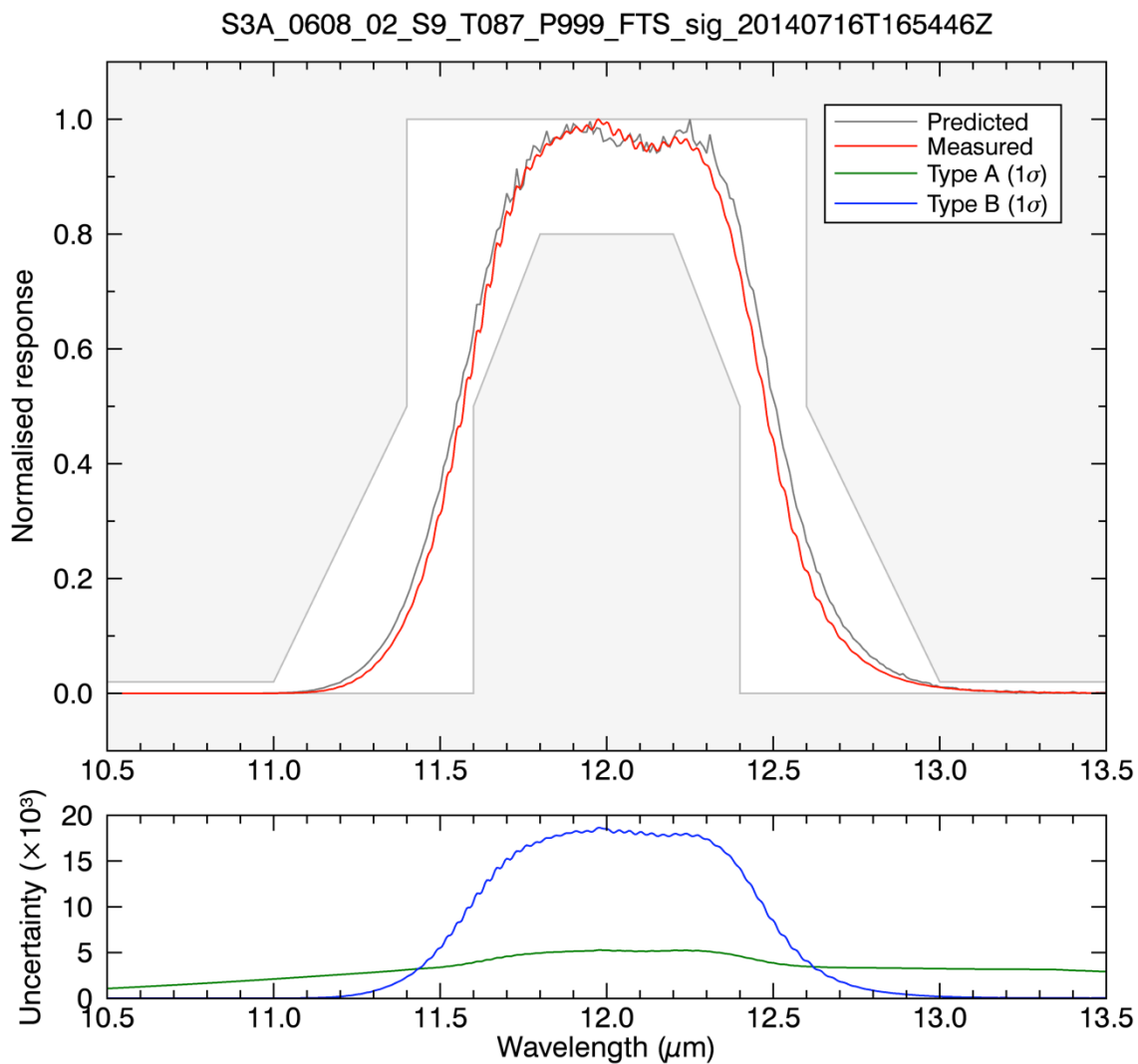


Figure 8.27 The normalised unpolarised spectral response of S9 detector 1 (analogue signal) at 87K.

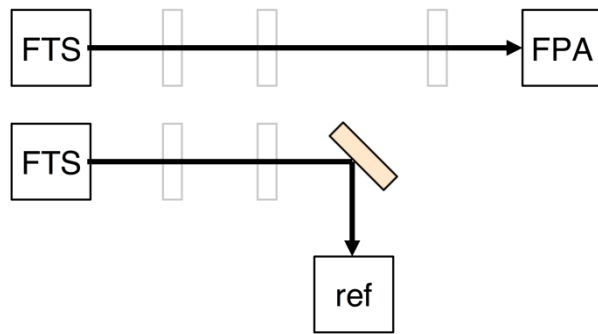


Figure 8.28 Spectrometer schematic setup for S9 FPA and reference measurements. No additional filters were installed.

8.5 FPA unpolarised spectral response temperature sensitivity

The unpolarised spectral response measurements of channels S4 – S9 were repeated at the planned FPA temperatures of 92 K and 100 K. An unplanned cooler event caused the FPA temperature to rise and the opportunity was taken to collect a further set of measurements at 103 K. Measurements of S1 – S3 were planned for 295 K only, however additional measurements were taken at other temperatures as the opportunity arose, including at 140 K while the FPA was cooling.

The results are presented in the following subsections. Each subsection summarises one channel and contains a single figure, except for S9 where the same data is plotted twice with different normalisation schemes.

8.5.1 S1 unpolarised spectral response temperature sensitivity

S3A_0802_01_S1_T087_P999_FTS_obs_20140718T155657Z S3A_0908_02_S1_T092_P999_FTS_obs_20140722T114630Z
S3A_0502_03_S1_T140_P999_FTS_sig_20140715T141228Z S3A_0102_01_S1_T295_P999_FTS_obs_20140711T163812Z

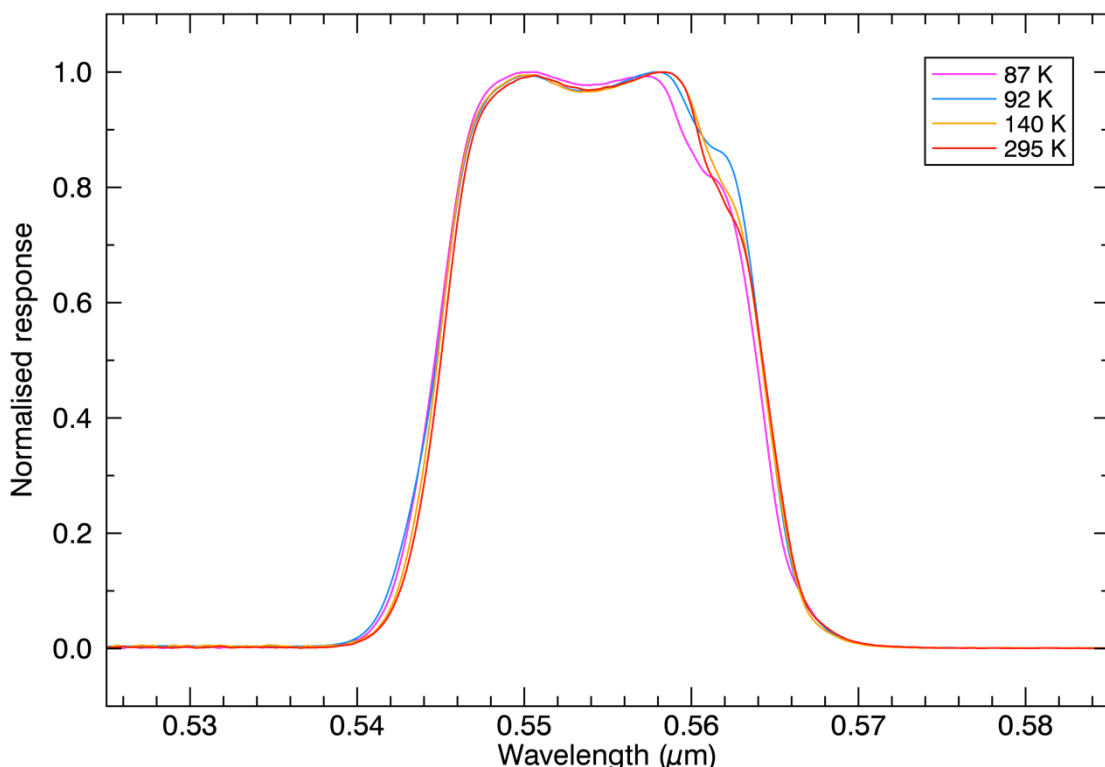


Figure 8.29 Temperature dependence of the unpolarised normalised response of S1 detector 1 (analogue signal).



8.5.2 S2 unpolarised spectral response temperature sensitivity

S3A_0805_01_S2_T087_P999_FTS_obs_20140718T162407Z S3A_0505_01_S2_T140_P999_FTS_sig_20140715T151555Z
S3A_0105_01_S2_T295_P999_FTS_obs_20140711T170022Z

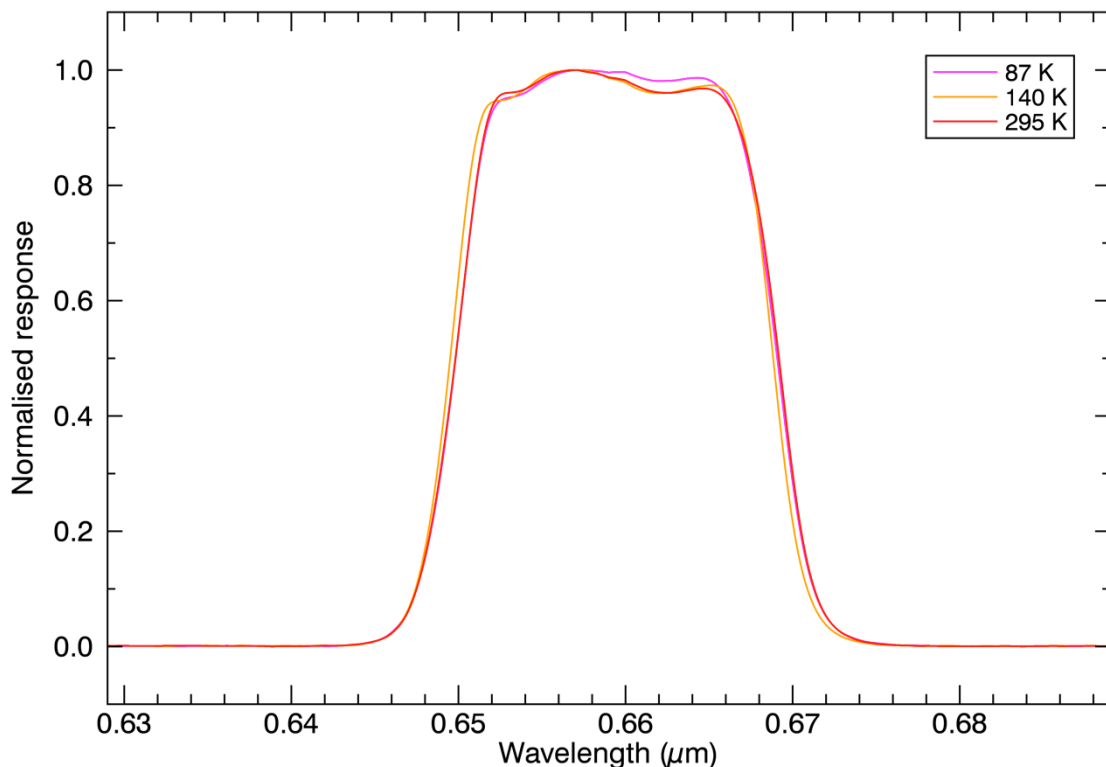


Figure 8.30 Temperature dependence of the unpolarised normalised response of S2 detector 1 (analogue signal).



8.5.3 S3 unpolarised spectral response temperature sensitivity

S3A_0808_01_S3_T087_P999_FTS_obs_20140718T164511Z S3A_0508_01_S3_T140_P999_FTS_sig_20140715T155007Z
S3A_0108_01_S3_T295_P999_FTS_obs_20140711T171328Z

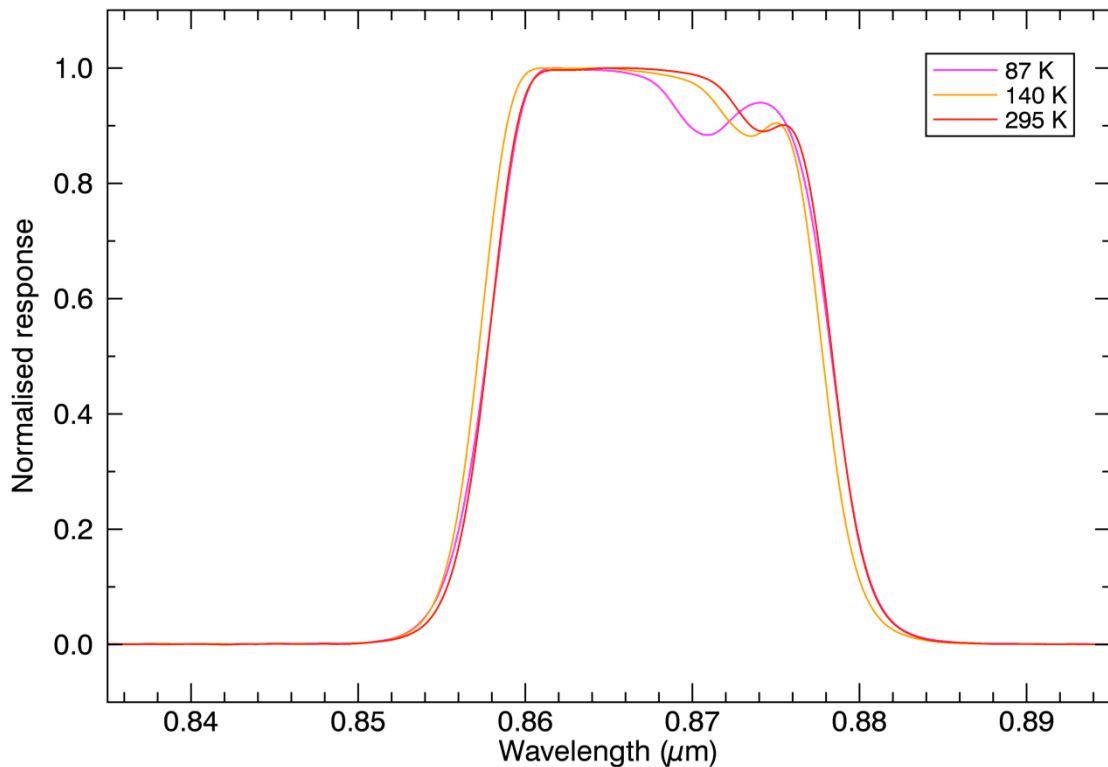


Figure 8.31 Temperature dependence of the unpolarised normalised response of S3 detector 1 (analogue signal).



8.5.4 S4 unpolarised spectral response temperature sensitivity

S3A_0202_01_S4_T087_P999_FTS_sig_20140717T170115Z S3A_0317_01_S4_T092_P999_FTS_sig_20140721T152506Z
S3A_0402_01_S4_T100_P999_FTS_sig_20140723T125217Z S3A_1005_01_S4_T103_P999_FTS_sig_20140724T170718Z

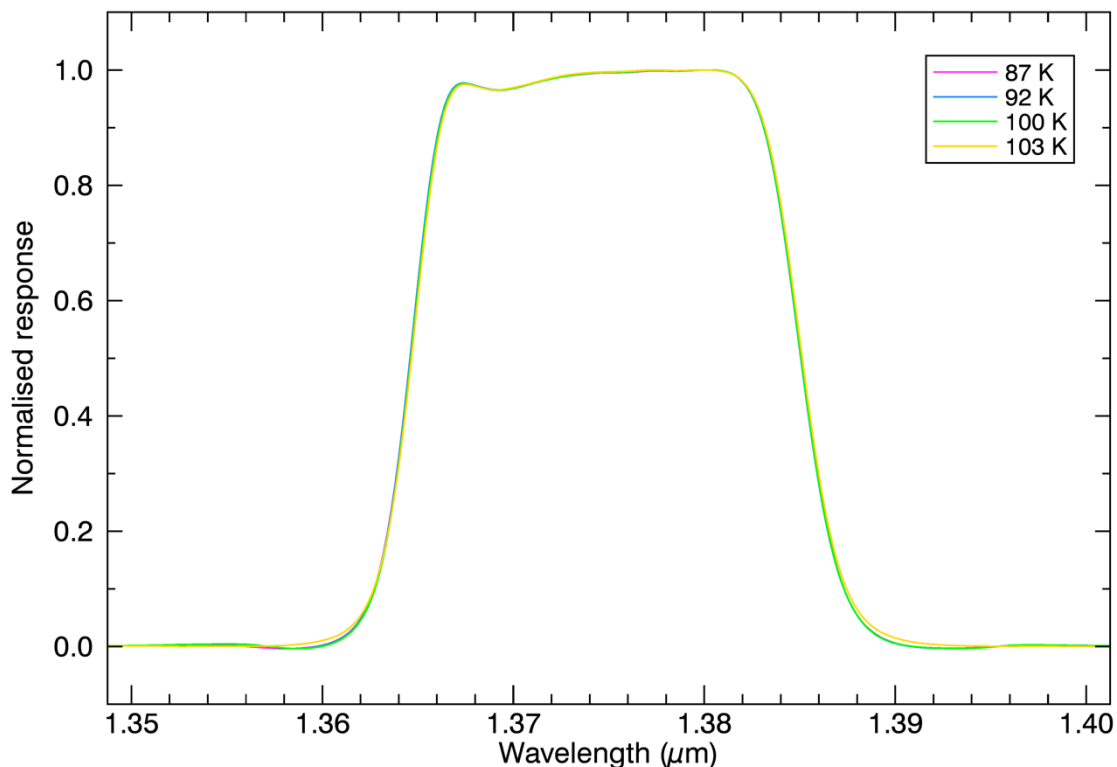


Figure 8.32 Temperature dependence of the unpolarised normalised response of S4 detector 1 (analogue signal).



8.5.5 S5 unpolarised spectral response temperature sensitivity

S3A_0205_01_S5_T087_P999_FTS_sig_20140717T173232Z S3A_0320_01_S5_T092_P999_FTS_sig_20140721T154647Z
S3A_0405_02_S5_T100_P999_FTS_sig_20140723T132213Z S3A_1008_01_S5_T103_P999_FTS_sig_20140724T182057Z

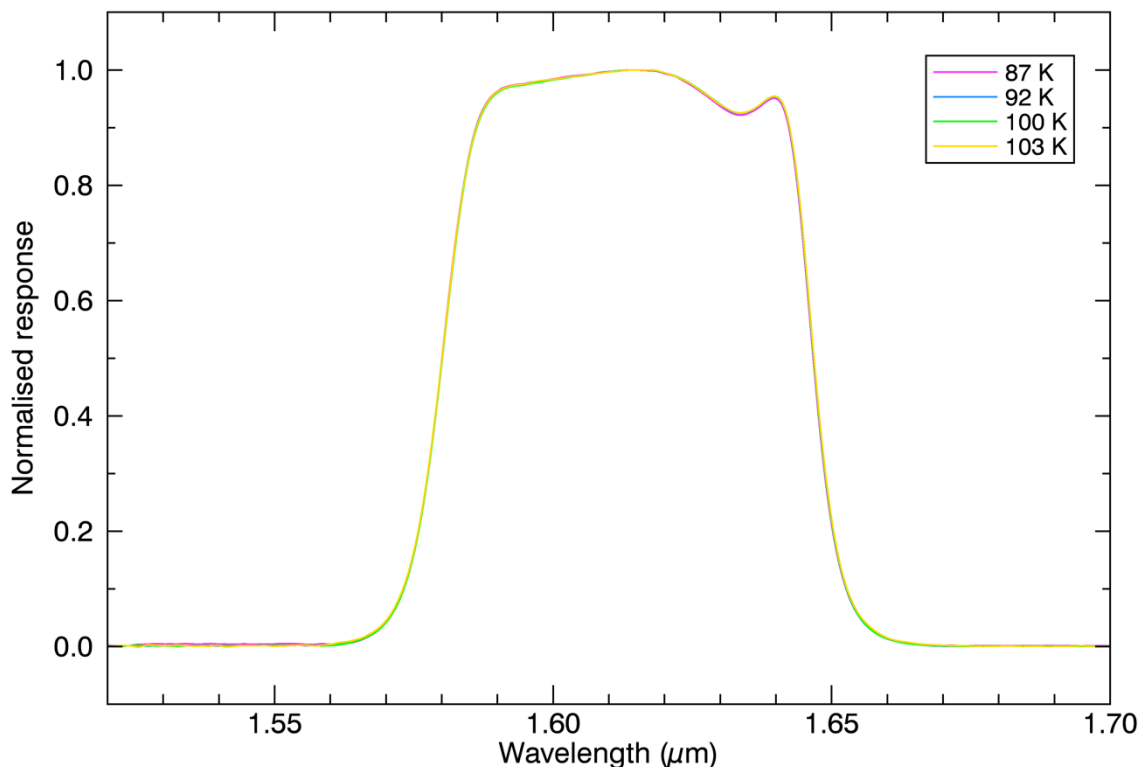


Figure 8.33 Temperature dependence of the unpolarised normalised response of S5 detector 1 (analogue signal).



8.5.6 S6 unpolarised spectral response temperature sensitivity

S3A_0208_01_S6_T087_P999_FTS_sig_20140717T174734Z S3A_0323_01_S6_T092_P999_FTS_sig_20140721T160040Z
S3A_0408_01_S6_T100_P999_FTS_sig_20140723T133744Z S3A_1011_01_S6_T103_P999_FTS_sig_20140724T174511Z

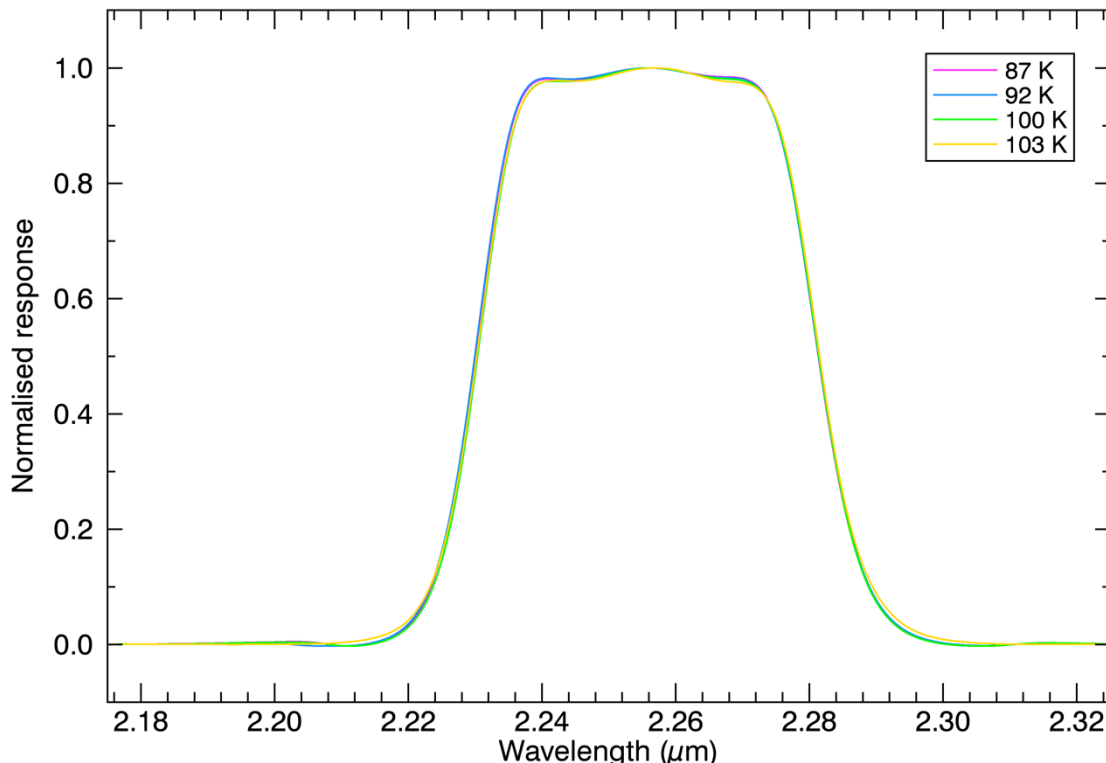


Figure 8.34 Temperature dependence of the unpolarised normalised response of S6 detector 1 (analogue signal).



8.5.7 S7 unpolarised spectral response temperature sensitivity

S3A_0602_03_S7_T087_P999_FTS_sig_20140717T115211Z S3A_0302_01_S7_T092_P999_FTS_sig_20140721T175757Z
S3A_0411_01_S7_T100_P999_FTS_sig_20140723T144126Z S3A_1014_02_S7_T103_P999_FTS_sig_20140725T112636Z

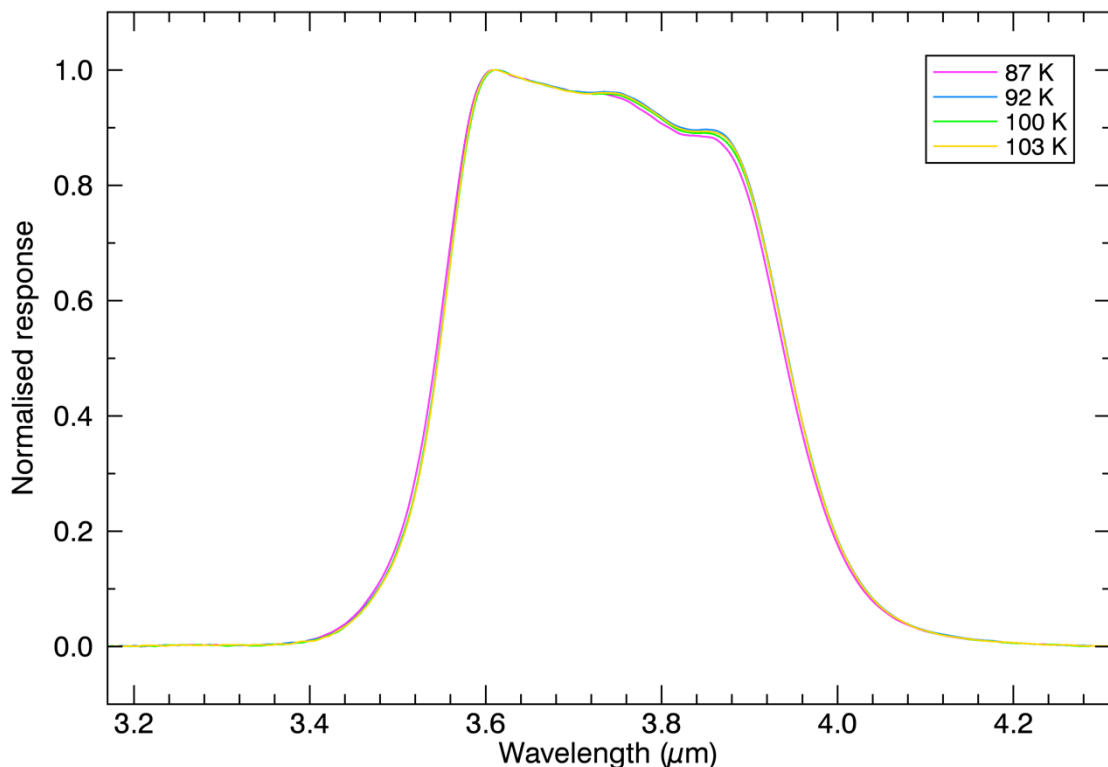


Figure 8.35 Temperature dependence of the unpolarised normalised response of S7 detector 1 (analogue signal).



8.5.8 S8 unpolarised spectral response temperature sensitivity

S3A_0605_01_S8_T087_P999_FTS_sig_20140716T162733Z S3A_0305_01_S8_T092_P999_FTS_sig_20140721T181941Z
S3A_0414_01_S8_T100_P999_FTS_sig_20140723T145803Z

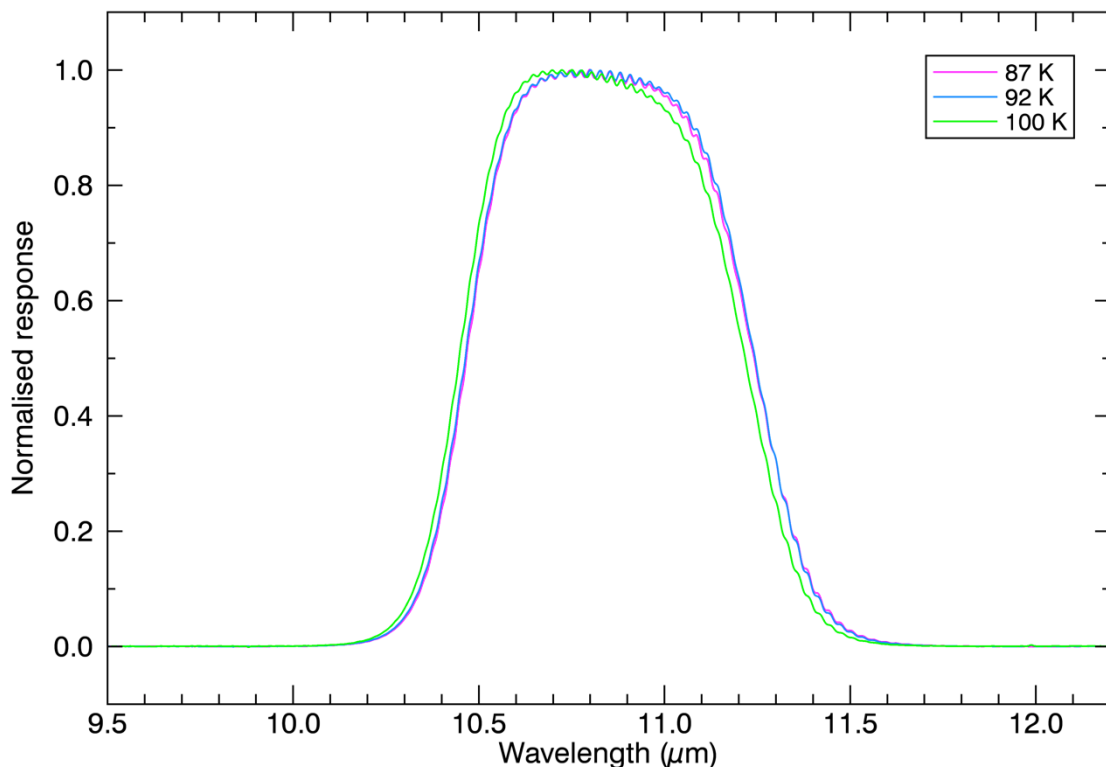


Figure 8.36 Temperature dependence of the unpolarised normalised response of S8 detector 1 (analogue signal).



8.5.9 S9 unpolarised spectral response temperature sensitivity

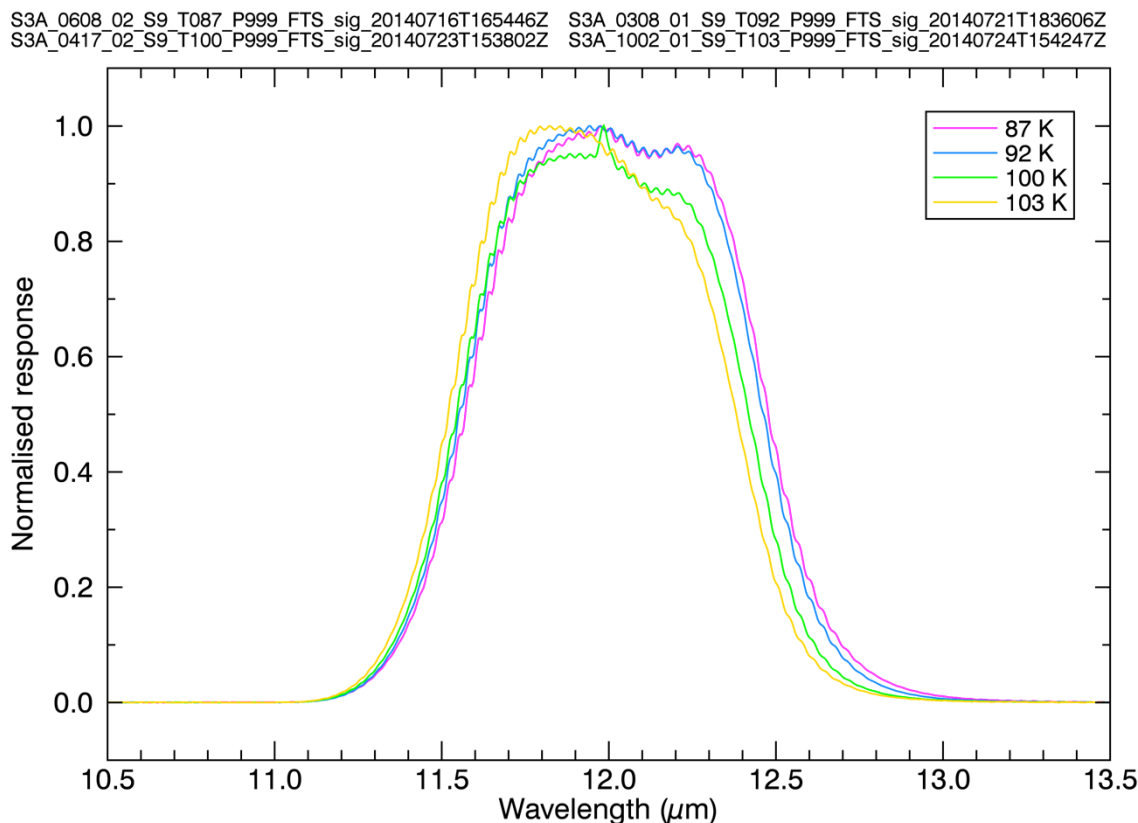


Figure 8.37 Temperature dependence of the unpolarised normalised response of S9 detector 1 (analogue signal).



SLSTR B FPA Spectral
Calibration Report

Date: 29-06-2015 Page 48 of 59

S3A_0608_02_S9_T087_P999_FTS_sig_20140716T165446Z S3A_0308_01_S9_T092_P999_FTS_sig_20140721T183606Z
S3A_0417_02_S9_T100_P999_FTS_sig_20140723T153802Z S3A_1002_01_S9_T103_P999_FTS_sig_20140724T154247Z

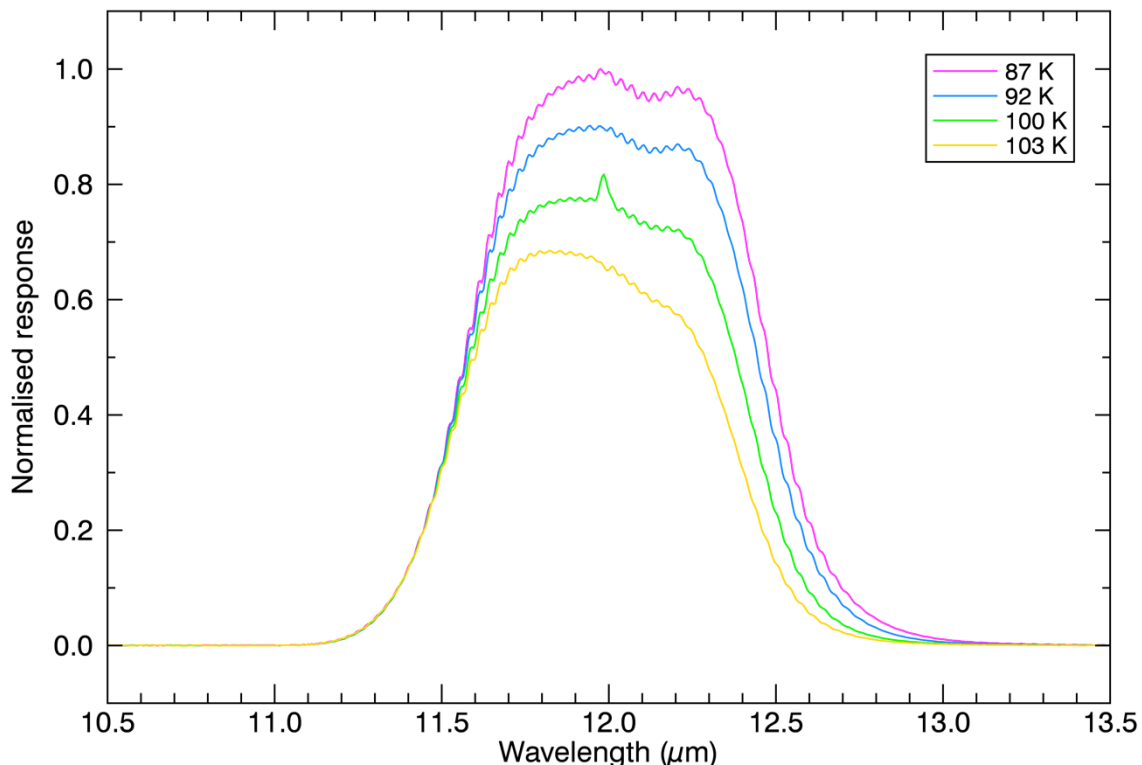


Figure 8.38 Temperature dependence of the unpolarised response of S9 detector 1 (analogue signal), normalised at 0.25 of the 87 K full scale signal on the shortwave edge

8.6 FPA unpolarised out-of-band responses at 87K

The User Requirements Document (URD) [AD 3] out-of-band response requirements do not specify source functions. These are critical to the assessment of the requirements. At one extreme, a very narrow source function centred at a detector's peak response would allow any channel to pass the requirement, regardless of the quality of its out-of-band blocking. This report assesses the URD requirements with a 5778 K Planck source, representing solar emission, for the reflectance channels (S1 – S6) and a 290 K Planck source, representing thermal emission from the earth, for the thermal channels (S7 – S9).

The spectrometer operates in wavelength bands limited by the spectral properties of its sources and optical components. Where there is little or no signal, measurement uncertainties dominate. If these regions were included in the out-of-band integrals specified in the requirements, the integrals could not meaningfully be evaluated. Where a channel's main response is pitched at some distance from the peak of the source function, uncertainties near to the source function peak are amplified. For some channels (e.g. to the longwave side of S7) this effect can be quite extreme.

Particular measurement constraints include:

S1 – S3: There is almost no system sensitivity below 500 nm as the spectrometer optics (gold coated mirrors) and the ZnSe vacuum window cut off, and the output of the quartz halogen lamp source (2800 K, emission peak at $\sim 1 \mu\text{m}$) drops rapidly. The silicon reference detector, against which the measurements are scaled, was calibrated up to 1.0 μm (and has a long wave cut off at 1.1 μm).

S4 – S6: There is minimal signal below 1 μm (CaF_2 beam splitter) or above 4 μm (quartz halogen lamp source). The calibrated spectral range of the DLATGS reference detector is limited to 0.9 μm . There are Fourier artefacts in the immediate wings of the in-band response, presumed to be due to the sampled nature of the analogue signal output from the EGSE in these channels. At the shortwave side of the main response, these features are amplified by the solar source function and these, combined with baseline errors, are sufficient to swamp the out-of-band integration.

S7: The S7 filter is pitched at some distance to the shortwave side of the peak of the 290 K source function and the radiance at the filter centre is only 3.3% (in units of $\text{W m}^{-2}\text{sr}^{-1}\mu\text{m}^{-1}$) of that at the peak. Consequently, longwave measurement uncertainties are grossly amplified.

S8 – S9: There are "classic" detector non-linearity Fourier artefacts at exactly twice the frequency (half the wavelength) of the main response, of order 1% of the amplitude of the main response. Integration of the short wave responses was truncated just above these features.

Typically, measurement uncertainties are of significant magnitude compared to the required 0.1% peak signal threshold and consequently the positions of these thresholds are difficult to identify. In this report, the signals in each wing of the detector response are integrated until they reach 0.5% of the total detected power (half of the requirement budget). If the detector signal exceeds 0.1% of the peak signal at these points in both wings, then the channel satisfies its requirement. This test is sufficient to demonstrate the requirement: that is, all the channels that satisfy this test also satisfy the requirement (although the reverse may not be true).

The results are summarised in Table 8.1. The results are conservative. The integrations include baseline errors associated with the measurement (which are always positive) and some small Fourier transform artefacts. The true performances of the channels are likely to exceed the tabulated values. The shortwave performance of S4 and S5 could not be determined from the laboratory measurements over any reasonable spectral range as measurement uncertainties dominated.

Channel	Source temperature	Integration range	Shortwave threshold	Longwave threshold
S1	5778 K	513 nm – 1,000 nm	5.36% @ 541 nm	4.39% @ 568 nm
S2	5778 K	570 nm – 1,000 nm	3.70% @ 646 nm	3.28% @ 673 nm
S3	5778 K	700 nm – 1,000 nm	0.14% @ 830 nm	5.80% @ 881 nm
S4	5778 K	1.1 µm – 3.8 µm	?	4.96% @ 1.388 µm
S5	5778 K	1.1 µm – 3.8 µm	?	2.58% @ 1.657 µm
S6	5778 K	1.7 µm – 2.8 µm	1.51% @ 2.218 µm	6.75% @ 2.290 µm
S7	290 K	1.0 µm – 5.0 µm	5.19% @ 3.48 µm	1.42% @ 4.19 µm
S8	290 K	5.8 µm – 20 µm	6.19% @ 10.31 µm	4.13% @ 11.46 µm
S9	290 K	6.5 µm – 20 µm	5.93% @ 11.31 µm	3.11% @ 12.84 µm

Table 8.1 Channel normalised responses at the thresholds on the shortwave and longwave response edges where the integrated detected power viewing a Planck source reaches 0.5% of the total detected power. The shortwave performances of S4 and S5 could not be determined over any reasonable integration range.

8.7 S8 longwave and S9 shortwave slopes at 87K

The “slopes” of the S8 shortwave edge and the S9 longwave edge (the intervals over which the channel responses changed from 5% to 80% of their peak values) were 0.325 µm (S8) and 0.384 µm (S9) for unpolarised measurements of the spectral responses at 87K.

9 Conclusions

A complete set of SLSTR B FPA spectral calibration measurements were successfully collected with a novel measurement technique, Fourier spectroscopy, which gave:

- Excellent spectral registration,
- High spectral resolution ($\sim 1 \text{ cm}^{-1}$ for all measurements),
- A high optical throughput,
- A fast measurement cycle (~ 15 minutes per channel, including reference measurements).

The fast measurement cycle was particularly useful for the optimisation of individual measurements and allowed additional measurements (e.g. cryogenic measurements for S1 – S3) to be inserted without undue impact on the schedule.

Nearly 400 separate measurements were made during the campaign. There were no FPA problems beyond an occasional cryocooler reset and only one other significant equipment failure – a DLATGS reference detector that was replaced with a backup unit. Code developed before the campaign to reformat FEE and data logger binary data worked without incident.

Good quality measurements were captured for all channels. With the exception of the out-of-band response characterisations, where there was not sufficient spectral coverage to assess the required integration range, all URD requirements have been addressed. We note that the spectral coverage problem is common to all spectrometer types as they share source and detector technologies. Only a few FPA non-compliances were identified, mostly minor. Compliance with the URD requirements is summarised in the Compliance Matrix (Section 10).

9.1 Lessons learned

Given the lack of a calibration rehearsal or test data, relatively few problems were encountered during the calibration campaign. The most significant were:

- Alignment: The wedged ZnSe window that separated the spectrometer and FPA vacuum spaces moved the spectrometer spot imaged on the FPA pupil, resulting in gross initial alignment errors, until the effect was understood and corrected with a wedged spacer. Smaller alignment changes between channels, due to the spectral dependence of the refractive index of the window material, required fine realignment with the steerable spectrometer final optics between each set of measurements.
- Fourier artefacts: There were artefacts due to the resampled nature of the analogue signals from channels S4 – S6 and, to a lesser extent, channel S7. There were also “classic” detector non-linearity artefacts in channels S8 and S9 at multiples of the detector centre frequencies.
- Responsivity mismatches: There was a significant mismatch between the responsivities of the longer wavelength channels, particularly S4 – S7, and the calibrated reference detector: This was resolved with neutral density filters. This problem is hard to avoid, regardless of spectrometer technology, as the gain of the reference detector must be very stable over long periods (weeks) both while being calibrated and during the measurement campaign. Only cooled semiconductor longwave detectors have responsivities comparable with the FPA detectors, but are very temperature sensitive and difficult to operate consistently over long periods.
- Baseline errors: While the performance of the Brucker IFS120 spectrometer is very good for this class of instrument and was adequate for the measurements, lower baseline errors would be desirable.

- The synchronisation data logger was free running, resulting in additional processing complexity for the digital FEE data.

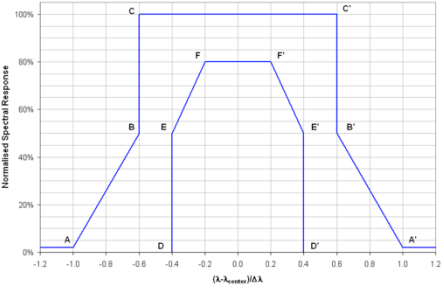
For future campaigns, the alignment problem will be addressed with a window that has a much less pronounced wedge and/or with additional compensating windows. The Fourier artefacts seen in channels S4 – S7 should not be present in the digital FEE data, however it is a significantly more complex problem to reconstruct interferograms and spectra from these data. Now that it is clear that digital timing pulses are available from the EGSE, it should be possible to sample the data logger synchronisation data synchronously with the FEE data.

We note that the FPA was not baked out before cooling. We think that this would be a worthwhile precaution before future measurements.

9.2 Outstanding work

- Polarisation measurements for channels S7 – S9: Additional measurements to characterise the spectrometer are now complete and a theoretical basis has been developed.
- Digital FEE data: Some processing tests have been made, but a robust semi-automated scheme is required to process the large number of data files.

10 Compliance matrix

Description	Compliance	Comment
S3-SL-URD-REQ-036 a		
The spectral response of the channels of the instrument normalised by its maximum shall meet the spectral template plotted in [AD 3] Figure 1. Note: These templates correspond to end-to-end performance, not just FPA and filters.	S1: compliant S2: compliant S3: not compliant S4: compliant S5: not compliant S6: not compliant S7: not compliant S8: compliant S9: compliant	~ 3 nm shift to longwave, both edges For S4 only, the URD gives filter width range (15 nm – 20 nm). Channel assessed against a 17.5 nm width. Marginal non-compliance at B' long wave template corner ([AD 3] Figure 1). Marginal non-compliance at B' long wave template corner ([AD 3] Figure 1). Marginal non-compliance at A' long wave template corner ([AD 3] Figure 1: 2.6% response measured, 2.0% required)
		
S3-SL-URD-REQ-037 a		
The relative spectral responses of all channels shall be known in flight to better than 5% of their peak response at any wavelength.	S1: compliant S2: compliant S3: compliant S4: compliant S5: compliant S6: compliant S7: compliant S8: compliant S9: compliant	
S3-SL-URD-REQ-038 a		
For any solar channel, the out-of-band integrated signal, as defined in the following equation, shall be less than 1% of the total integrated signal.	S1: compliant * S2: compliant * S3: compliant * S4: LW compliant *, SW not determined S5: LW compliant *, SW not determined S6: compliant *	513 nm – 1000 nm integration range 570 nm – 1000 nm integration range 700 nm – 1000 nm integration range 1.1 μm – 3.8 μm integration range 1.1 μm – 3.8 μm integration range 1.7 μm – 2.8 μm integration range
$1 - \frac{\int_{\lambda_{\min}}^{\lambda_{\max}} L(\lambda)R(\lambda)d\lambda}{\int_{0.3\mu m}^{2.0\mu m} L(\lambda)R(\lambda)d\lambda} < 0.01$ <p>where λ_{\max} and λ_{\min} are the wavelengths at which the measured response has reached 0.1% of the</p>		* The source function $L(\lambda)$ is not defined. This function has a critical impact on the assessment of the requirement. A Planck

**SLSTR B FPA Spectral
Calibration Report**

Date: 29-06-2015 Page 54 of 59

Description	Compliance	Comment
maximum channel response. The integrated signal corresponds to end-to-end system performance including spectral filters and detectors.		source at 5778 K representing solar emission was chosen. Assessment could not be performed over the full wavelength range (0.3 μm – 20 μm) for two reasons: a) The spectrometer operates in wavelength bands limited by the spectral properties of its sources and optical components. Where there is little or no signal, measurement uncertainties dominate. If these regions were included in the integrals, the integrals could not meaningfully be evaluated. b) The reference detectors could not be calibrated over the full spectral range.
S3-SL-URD-REQ-575		
For any thermal channel, the out-of-band integrated signal, as defined in the following equation, shall be less than 1 % (goal 0.01 %) of the total integrated signal $1 - \frac{\int_{\lambda_{\min}}^{\lambda_{\max}} L(\lambda)R(\lambda)d\lambda}{\int_{0.3\mu m}^{20\mu m} L(\lambda)R(\lambda)d\lambda} < 1\% \text{ (goal: 0.01\%)}$ where λ_{\max} and λ_{\min} are the wavelengths at which the measured response has reached 0.1% of the maximum channel response. The integrated signal corresponds to end-to-end system performance including spectral filters and detectors.	S7: compliant * S8: compliant * S9: compliant *	1.0 μm – 5.0 μm integration range 5.8 μm – 20 μm integration range 6.5 μm – 20 μm integration range * The source function $L(\lambda)$ is not defined. This function has a critical impact on the assessment of the requirement. A Planck source at 290 K representing terrestrial emission was chosen. Assessment could not be performed over the full wavelength range (0.3 μm – 20 μm) for two reasons: a) The spectrometer operates in wavelength bands limited by the spectral properties of its sources and optical components. Where there is little or no signal, measurement uncertainties dominate. If these regions were included in the integrals, the integrals could not meaningfully be evaluated. b) The reference detector could not be calibrated over the full spectral range.
S3-SL-URD-REQ-599		
The “80% – 5% slope” of channel S8 on the long wavelength side of the spectral response curve shall be lower than 0.34 μm.	compliant	0.325 μm measured
S3-SL-URD-REQ-600		
The “80% – 5% slope” of channel S9 on the short wavelength side of the spectral response curve shall be lower than 0.37 μm.	not compliant	0.384 μm measured

**SLSTR B FPA Spectral
Calibration Report**

Date: 29-06-2015 Page 55 of 59

Description	Compliance	Comment
S3-SL-URD-REQ-060 (thermal channels)		
SLSTR polarisation sensitivity shall be in average less than 0.10 in the thermal channels (MWIR, LWIR). Performance shall be known to better than 0.5%.	S7: TBC	
	S8: TBC	
	S9: TBC	
S3-SL-URD-REQ-090a (spectral response)		
Instrument normalised spectral response $R(\lambda)$. Values to be provided for all spectral channels as a function of wavelength over the minimum range $[\lambda_{\text{center}} - \Delta\lambda 50\%, \lambda_{\text{center}} + \Delta\lambda 50\%]$, up to λ_{\min} & λ_{\max} for which normalised spectral response is below 0.1%. These measurements shall be performed at least at integrated FPA level.	S1: compliant	
	S2: compliant	
	S3: compliant	
	S4: compliant	
	S5: compliant	
	S6: compliant	
	S7: compliant	
	S8: compliant	
	S9: compliant	
S3-SL-URD-REQ-090a (polarisation sensitivity, thermal channels)		
Sensitivity of the instrument on the polarisation of the incident electromagnetic radiation. Values to be provided for both views for the edge pixels and central pixel and for all spectral channels. Polarisation shall be characterized within complete views, and including calibration views with an accuracy of 0.5 %. In the solar channels, these measurements shall be performed at integrated instrument level. In the thermal channels, these measurements shall be performed at integrated FPA level at least.	S7: TBC	
	S8: TBC	
	S9: TBC	



11 Appendix

11.1 File naming

All files generated as a part of the FPA spectral calibration campaign follow broadly the same file naming convention. The body of the file name is 49 characters long and contains nine fixed-width, underscore ("_") delimited fields which identify the channel under test, the spectrometer configuration and the time of measurement.

11.1.1 FEE binary spectrogram file

An FEE binary spectrogram file contains a dump of the raw binary data stream generated by the FPA EGSE when the FPA is attached to the Brucker IFS-120 spectrometer and observes a series of spectrograms for the conditions identified in the file name. The file name has format:

S3x_iiii_jj_Ss_Tttt_Pppp_FEE_mmm_yyyyymmddThhmmssZ.Nn.bin

and is stored in subdirectory :

S3x_iiii_jj_Ss_Tttt_Pppp_FEE_mmm_yyyyymmddThhmmssZ/Data

where:

x = platform identifier ("A", "B", ... , one letter)

iiii = measurement sequence identifier ("1" and up, four digits)

jj = measurement sub-sequence identifier ("1" and up, two digits)

s = channel identifier ("1" – "9", one digit)

ttt = notional FPA operating temperature ("087", "092", "100", "295", "999" = N/A, three digits)

ppp = polariser angle ("000", "060", "120", "999" = none, three digits)

mmm = measurement type (three letters):

"sig" = FPA detector signal

"obs" = out-of-band FPA detector signal

yyyyymmdd = UTC file start date (year, month, day; four + two + two digits)

hhmmss = UTC file start time (hour, minute, second; two + two + two digits)

n = FEE file counter (one digit)

11.1.2 FEE ASCII spectrogram file

An FEE ASCII spectrogram data file contains a simple text extraction from the corresponding binary data file (Section 11.1.1) consisting of signal counts for all of the detectors associated with the instrument channel identified in the file name. The file name has format:

S3x_iiii_jj_Ss_Tttt_Pppp_FEE_mmm_yyyyymmddThhmmssZ.dat

where:

x = platform identifier ("A", "B", ... , one letter)

iiii = measurement sequence identifier ("1" and up, four digits)

jj = measurement sub-sequence identifier ("1" and up, two digits)

s = channel identifier ("1" – "9", one digit)

t_{ttt} = notional FPA operating temperature ("087", "092", "100", "295", "999" = N/A, three digits)

ppp = polariser angle ("000", "060", "120", "999" = none, three digits)

mmm = measurement type (three letters):

"sig" = FPA detector signal

"obs" = out-of-band FPA detector signal

yyyyymmdd = UTC file start date (year, month, day; four + two + two digits)

hhmmss = UTC file start time (hour, minute, second; two + two + two digits)

11.1.3 Brucker OPUS spectrogram file

A Brucker OPUS spectrogram file is encoded in OPUS format and contains both a spectrogram recorded with the Brucker IFS-120 spectrometer's native data acquisition hardware and a spectral profile derived from the spectrogram. The signal can originate either from a Brucker internal detector or from an analogue FPA detector output. The file name has format:

`S3x_iiii_jj_Ss_Tttt_Pppp_FTS_mmm_yyyyymmddThhmmssZ.k`

where:

`x` = platform identifier ("A", "B", ... , one letter)

`iiii` = measurement sequence identifier ("1" and up, four digits)

`jj` = measurement sub-sequence identifier ("1" and up, two digits)

`s` = channel or group identifier ("1" – "9", "V" = visible, "S" = SWIR, "T" = TIR, one character)

`ttt` = notional FPA operating temperature ("087", "092", "100", "295", "999" = N/A, three digits)

`ppp` = polariser angle ("000", "060", "120", "999" = none, three digits)

`mmm` = measurement type (three letters):

"`sig`" = FPA detector signal

"`ref`" = spectrometer reference signal

"`obs`" = out-of-band FPA detector signal

"`obr`" = out-of-band spectrometer reference signal

"`sga`" = turn-and-turn-about test, "A" detector in signal position

"`sgb`" = turn-and-turn-about test, "B" detector in signal position

"`rfa`" = turn-and-turn-about test, "A" detector in reference position

"`rfb`" = turn-and-turn-about test, "B" detector in reference position

"`tst`" = test file that does not form a part of the core measurement series

`yyyyymmdd` = UTC file start date (year, month, day; four + two + two digits)

`hhmmss` = UTC file start time (hour, minute, second; two + two + two digits)

`k` = scan number ("0" and up, one or more digits)

11.1.4 National Instruments TDMS synchronisation file

A National Instruments TDMS synchronisation file is encoded in TDMS format and contains laser fringe and spectrogram centre burst synchronisation data captured with a NI data logger. The file name has format:

`S3x_iiii_jj_Ss_Tttt_Pppp_syn_mmm_yyyyymmddThhmmssZ.tdms`

where:

`x` = platform identifier ("A", "B", ... , one letter)

`iiii` = measurement sequence identifier ("1" and up, four digits)

`jj` = measurement sub-sequence identifier ("1" and up, two digits)

`s` = channel identifier ("1" – "9", one digit)

`tttt` = notional FPA operating temperature ("087", "092", "100", "295", "999" = N/A, three digits)

`ppp` = polariser angle ("000", "060", "120", "999" = none, three digits)

`mmm` = measurement type (three letters):

"sig" = FPA measurement

"obs" = out-of-band FPA measurement

`yyyyymmdd` = UTC file start date (year, month, day; four + two + two digits)

`hhmmss` = UTC file start time (hour, minute, second; two + two + two digits)

11.1.5 National Instruments netCDF synchronisation file

A National Instruments netCDF synchronisation file is encoded in netCDF4 format and contains reformatted information extracted from the corresponding TDMS file (Section 11.1.4). The file name has format:

`S3x_iiii_jj_Ss_Tttt_Pppp_syn_mmm_yyyyymmddThhmmssZ.nc`

where:

`x` = platform identifier ("A", "B", ... , one letter)

`iiii` = measurement sequence identifier ("1" and up, four digits)

`jj` = measurement sub-sequence identifier ("1" and up, two digits)

`s` = channel identifier ("1" – "9", one digit)

`tttt` = notional FPA operating temperature ("087", "092", "100", "295", "999" = N/A, three digits)

`ppp` = polariser angle ("000", "060", "120", "999" = none, three digits)

`mmm` = measurement type (three letters):

"sig" = FPA measurement

"obs" = out-of-band FPA measurement

`yyyyymmdd` = UTC file start date (year, month, day; four + two + two digits)

`hhmmss` = UTC file start time (hour, minute, second; two + two + two digits)